

**Astrocyte and oligodendrocyte dynamics in central pontine
myelinolysis**

Academic Dissertation

submitted in fulfillment of the requirements for the degree of doctor of medicine

Dr. med.

an der Medizinischen Fakultät
der Universität Leipzig

eingereicht von

Ronja Löber-Handwerker (geb. Handwerker), 24.12.1990, geboren in Duisburg

Identification: dok-med-3114

angefertigt an der

Medizinischen Fakultät der Universität Leipzig, Abteilung Neuropathologie, Leipzig

Betreuer

Prof. Dr. med. Wolf C. Müller

Dr. med. Alonso Barrantes- Freer

Beschluss über die Verleihung des Doktorgrades vom 06.07.2022.

Abstract

Introduction: Astrocytopathy is known to be an early feature of different neuroinflammatory diseases. However, the impact of astrocyte loss and repopulation on the development and progression of demyelinating lesions in complex etiologies, such as multiple sclerosis, is difficult to determine. To more easily analyse astrocyte-oligodendrocyte-interactions during lesion formation and progression in the human brain, diseases like Central pontine myelinolysis (CPM) can be used as a less complex model of demyelinating disorders. CPM is a rare neurological condition characterized by damage to the myelin sheath of pontine nerves after osmotic shifts in serum. Astrocytopathy is regarded to be the first event in the pathogenesis of CPM lesions.

Methods: Histological investigation of autopsy tissue from human CPM patients was performed. Lesions were staged considering the myelination and the appearance of different astrocyte subtypes, which was used to judge behaviour of the astrocytic compartment. Further, dynamics of oligodendrocyte loss and repopulation were analysed and compared to the astrocytic repopulation.

Results: *Early-staged* lesions were largely demyelinated and showed an overall reduction of astrocyte densities. The few astrocytes present showed a bipolar morphology and were AQP4-negative, indicating an immature state. *Intermediate-stage* lesions were still largely demyelinated, but had increased overall densities of astrocytes, which did not yet reflect densities observed in the perilesion. Astrocytes appeared mostly ramified and AQP4-positive, indicating maturity. Nevertheless, bipolar astrocytes were still observable, indicating that repopulation was not yet finalized. *Late-stage* CPM-lesions were at least partially remyelinated. Astrocytes

were detectable in overall densities comparable to the perilesion and showed a ramified (or even reactive morphology), as well as regular expression of AQP4.

Investigating the oligodendrocytes, intralésional densities were reduced in early- and intermediate-stage lesions when compared to the perilesion. Re-increase in oligodendrocyte densities was first observable in late-stage lesions, but did not reach perilesional levels.

Conclusion: The study at hand indicates that the recovery of demyelinated osmolyte-induced pontine lesions follows a distinct time-course. Repopulation of the lesion with oligodendrocytes is not carried out until lesions are completely repopulated with functional resident astrocytes, as indicated by the ramified morphology and the expression of AQP4.

Further studies will be needed to determine, whether the appearance of immature astrocytes, indicating an ongoing repopulation of lesions with astrocytes, correlates with an inefficient repair of demyelinated lesions.

Table of Contents

List of Abbreviations.....	6
1 Introduction.....	7
1.1 Osmotic Demyelinating Syndrome.....	7
1.2 Clinical manifestation.....	9
1.3 Diagnosis and Management of CPM.....	11
1.4 Aetiology of Central Pontine Myelinolysis.....	14
1.5 The brain, its adaptation to hyponatraemia and response to correction – pathophysiology of CPM.....	16
1.6 Pathology of myelin.....	19
1.6.1 Astrocytopathy and oligodendrocytopathy.....	20
1.7 Aims of the study.....	23
2 Material und Methods.....	24
2.1 Patient tissue.....	24
2.2 Histology and immunohistochemistry.....	24
2.2.1 Basic concepts.....	24
2.2.2 Hematoxylin and Eosin (HE).....	26
2.2.3 Luxol Fast Blue/ Periodic Acid Schiff stain.....	27
2.2.4 Immunohistochemistry. Application and Protocol.....	28
2.3 Implementation.....	31
2.4 Estimation of demyelination.....	32
2.5 Analysis of cell density and proliferation.....	32
2.6 Data plotting and statistical analysis.....	32
3 Results.....	33
3.1 Patient cohort.....	33
3.2 Characteristics of demyelination.....	35
3.3 CPM lesion and disease staging.....	37

3.4	Astrocytes within human CPM lesions.....	42
3.4.1	Astrocyte densities are decreased in early CPM lesions.....	42
3.4.2	Astrocytes in CPM– morphological distinctions.....	45
3.5	Oligodendrocyte densities within human CPM lesions.....	48
3.6	Macrophages and activated microglia.....	54
3.6.1	KiM1P – a marker for infiltrating macrophages and activated microglia.....	54
3.6.2	Proliferating Iba1+ cells are observed in all lesion stages.....	58
4	Discussion.....	61
4.1	Lesion Staging.....	61
4.2	Astrocytes in the pathogenesis of CPM.....	65
4.3	Oligodendrocyte pathology in CPM.....	69
4.4	Mechanisms of regeneration in human CPM lesions.....	72
4.5	Summary, interpretation and limitations of our study.....	78
5	Conclusion and Outlook.....	80
6	Bibliography.....	82
7	List of Tables.....	91
8	List of Figures.....	92
9	Appendix.....	94
9.1	Declaration of Authenticity.....	94
9.2	Acknowledgements.....	95
9.3	Curriculum Vitae.....	95

List of Abbreviations

AQP4	Aquaporin 4
BBB	Blood-brain barrier
BDNF	Brain-derived neurotrophic factor
CPM	Central Pontine Myelinolysis
DAB	25 mg of 3,3-diaminobenzidine
EAE	Experimental autoimmune encephalomyelitis
EPM	Extra Pontine Myelinolysis
ET-1	Astrocyte-derived endothelin-1
FCS	Fetal calf serum
Gal-3	Galectin 3
GCS	Glasgow Coma Scale
GFAP	Glial fibrillary acidic protein
HE	Haematoxylin and Eosin
Iba1	Ionized calcium-binding adaptor molecule
IGF-1	Insulin-like growth factor-1
IHC	Immunohistochemistry
IL-1 β	Interleukin 1 beta
iNOS	Inducible nitric oxide synthase
KiM1P	Marker for macrophages/activated microglial cells
Ki67	Marker for cell proliferation and growth
LIF	Leukaemia inhibitory factor
MAG	Myelin-associated glycoprotein
MBP	Myelin basic protein
MOG	Myelin oligodendrocyte glycoprotein
ODS	Osmotic demyelination Syndrome
OPC	Oligodendrocyte progenitor cell
PDGF-A	Platelet-derived growth factor-A
PLP	Proteolipid protein
P25	Marker for oligodendroglial cells
TIMP-1	Tissue inhibitor of metalloproteinases-1
TNF	Tumour necrosis factor

1 Introduction

The brain is vulnerable, especially to metabolic stresses. The easiest way to wrap one's head around this intuitive yet very complex concept is from a clinical perspective. Thinking about hypoglycaemia, for example, with glucose being the number one fuel of brain cells, one realizes that even a slight fall in glucose may precipitate profound neurological dysfunction spanning slight confusion up until seizures, coma and death in severe cases (Ashrafian & Davey, 2001; De Felice & Lourenco, 2015). However, other metabolic disturbances have been linked to neurodegenerative, neuro-inflammatory, and possibly even psychiatric diseases (Saia-Cereda et al., 2017). One of the yet relatively poorly understood conditions with a recognized link to damage to the brain tissue due to metabolic insults is the Osmotic Demyelination Syndrome (ODS) encompassing Central Pontine Myelinolysis (CPM) and Extra Pontine Myelinolysis (EPM).

1.1 Osmotic Demyelinating Syndrome

CPM, as part of ODS, is a mostly unexplored non-primary neurological condition characterized by damage to the insulating myelin sheath of nerves. Over decades, CPM was considered extremely rare and inevitably fatal. With an estimated incidence of about 3 per 1000, Central Pontine Myelinolysis can, indeed, be considered a relatively rare condition. As a rare neurological phenomenon, it might often be suspected clinically but confirmed only at autopsy (Brown, 2000). The descriptive term "Osmotic Demyelination Syndrome" hints at the most common predisposing mechanism: an osmotic insult to the panglial syncytium. Primarily, ODS is associated with a rapid

correction of sodium concentration following hyponatraemia over a prolonged period of time (Bouchat et al., 2018; Singh et al., 2014). Areas particularly susceptible to myelinolysis include the brain stem and, importantly, the central pons, possibly due to a higher sensitivity of the pontine white and grey matter to electrolyte disturbances. Lesions outside these regions can also be found in some individuals and are not an uncommon phenomenon, referred to as “Extra Pontine Myelinolysis.” It is estimated that around 10% of patients with CPM also have EPM lesions in their CNS (Brown, 2000; Singh et al., 2014). One recently published paper compared cortical MS- with CPM/EPM lesions. In line with the literature they could demonstrate EPM lesions in one of their six CPM cases studied. These extrapontine lesions also showed demyelinated areas with myelin loss and preserved axonal structures, demonstrated multiple foamy macrophages as well as inflammatory cells and predominantly affected the cortex. They could also demonstrate that even though there are multiple similarities between demyelinating diseases e.g. the presence of markers for oxidative stress and ROS, each disease seems to have their somewhat disease specific milieu of cytokines, immune- and glial cells as well as neurons. Also the individual genetic background seems to play a major part in the development of specific lesions as the genes predict the cellular composition of each patient and thus the microenvironment in which lesions form (Junker et al., 2020).

ODS was first described by Adams et al. in 1959, who found morphological changes in centro-pontine regions of brains studied post-mortem of four patients dying from complications of malnutrition and alcoholism and presenting with pseudobulbar palsy and quadriplegia (Adams et al., 1959). The lesions found were described as spreading out from the basis pontis in a “Batwing shape” and appeared to be sharply

demarcated with relative sparing of corticobulbar-/spinal tracts (Adams et al., 1959; Kleinschmidt-Demasters et al., 2006; Tomlinson et al., 1976). In the 1970s, it was hypothesized that CPM resulted from a “special metabolic susceptibility of oligodendroglial cells in areas where neurons, glial cells, and myelin sheaths lie in close proximity to one another” (Tomlinson et al., 1976). This hypothesis was further concretized and experimentally confirmed by Kleinschmidt-DeMasters and Norenberg in 1981, who analysed blood samples from symptomatic ODS patients (Kleinschmidt-DeMasters & Norenberg, 1981). Also, it could be shown that induction of hyponatremia and subsequent rapid correction causes CPM-like lesions in animal studies (Bouchat et al., 2018; Illowsky & Laureno, 1987; Karp & Laureno, 1993; Kleinschmidt-DeMasters & Norenberg, 1981; R. Laureno & Karp, 1997; Laureno, 1983). These findings had a massive impact on modern medical practice as they, among others, led to the formulation and implementation of guidelines for management, correction, and prevention of hyponatremia in hospital patients via tight control of plasma sodium levels (Spasovski et al., 2014).

1.2 Clinical manifestation

Patients present with CPM most commonly between the ages of 30 and 60 years, and over half of the cases are found in male patients (Singh et al., 2014). Manifestation of CPM tends to run a biphasic course, with initial encephalopathy or seizures, followed by mild and short recovery and then rapid, severe deterioration. Nevertheless, like the outcome of the condition, the clinical manifestation is highly variable, ranging from no symptoms or signs to seizures, personality changes, coma, or locked-in-syndrome depending on the involvement of different parts or the presence of extra pontine lesions. All of these have been reported within only a few days of

recovery from hyponatraemia (Adams et al., 1959; Alleman, 2014; Graff-Radford et al., 2011; P. J. Martin & Young, 1995; Singh et al., 2014). Additionally, it seems that patients suffering acute hyponatraemia with development in under 48 hours present with more critical symptoms than patients in which hyponatraemia develops more slowly. On the other hand, hyponatraemia that develops chronically may predispose more commonly to the development of CPM when corrected (Hurley et al., 2011; Lien & Shapiro, 2007; Norenberg, 2010). The symptoms accurately reflect the fibre tracts involved and often represent the beginning of the second phase of the biphasic course: dysphagia and dysarthria, reflecting the involvement of the corticobulbar tract, flaccid quadriparesis reflecting demyelination of the corticospinal tract which later turns into spastic quadriparesis. Should the lesion become even bigger and involve the tegmentum of the pons, the patient may also present with oculomotor or pupillary involvement. Extra pontine lesions may dilute the clinical picture further as patients may present with psychiatric conditions or behavioural changes (R. J. Martin, 2004).

Even if knowledge about the disease has exponentially risen over the last decades, it is still not possible to safely predict the clinical outcome of a patient presenting with CPM. While a proportion of patients will fully recover, some will go on to have persistent neurological disabilities. Others will die from the disease. Even though the exact factors leading to recovery or death are matter of speculation, there seem to be factors associated with a more favourable rate of recovery. According to Kallakatta et al., these were among others: a higher Glasgow Coma Scale (GCS), less severe hyponatraemia and absence of other electrolyte disturbances like hypokalaemia. The team, however, also found factors that predispose to a less satisfactory prognosis

like post-liver transplantation or patients suffering from liver cirrhosis (Kallakatta et al., 2011). Other groups supported this idea of co-factors influencing the outcome of CPM (Bronster et al., 2000; de Morais et al., 2009; Kallakatta et al., 2011; Mochizuki et al., 2003; Singh et al., 2014; Yu et al., 2004). A systematic review of CPM from 2014 by Singh et al. found distinct differences between cases of CPM in patients following liver transplant and the “standard” CPM patient. They found that patients having had a liver transplant were more frequently male and had an underlying liver cirrhosis. Further, the demyelination seemed to be restricted to the pons, and they did present more frequently with seizures and encephalopathy but less often reported alcohol abuse and hyponatraemia. The study failed to give an explanation for the described phenomenon but proposed the idea of worse comorbidities or more severe demyelination within this subgroup. Post-mortem studies estimate a prevalence of up to 30% in the subset of patients with liver transplants and possibly a much higher number of undiagnosed cases (Singh et al., 2014).

1.3 Diagnosis and Management of CPM

When CPM was initially described in the 1960s, it was believed to have a worse outcome generally, since diagnosis could only be made by post-mortem autopsy findings. With growing awareness, knowledge about and availability of radiological diagnosis, as well as intense research over the past decades, mortality from CPM has continuously decreased, and good recovery may be achieved in about half of patients; excluding patients with concurrent liver transplantation (Graff-Radford et al., 2011; Kallakatta et al., 2011; Menger & Jorg, 1999; Singh et al., 2014). However, effective therapeutic interventions are yet to be found. This is mainly due to mostly late presentation, and difficulty of early diagnosis as focal pontine features of CPM

are an exception rather than the rule. It is, therefore, understandable that definitive ante-mortem diagnosis used to be impossible before utilization of radiological imaging (especially MRI). Nowadays, neuroimaging (MRI and CT) is the standard method for the ante-mortem diagnosis of ODS, and other possible diagnostic methods like diffusion-imaging are being evaluated.

Criteria like:

- Restricted diffusion in (extra-) pontine lesions
- Contrast enhancement (low T1 and high T2 signal intensity)
- Lesion location
- Lesion volume

are taken into account when evaluating an MRI of a patient with suspected CPM. New insights into the pathophysiology and advancements in CT and MRI diagnostics shine new light onto patients with classical appearance of pontine lesions on MRI but without or only diffuse clinical manifestation. These patients represent the sub-clinical spectrum of the condition (Kleinschmidt-DeMasters, Anderson, & Rubinstein, 1997; Mochizuki et al., 2003; Uchino et al., 2003). Interestingly, the presumed severity seen on CT or MRI does not seem to correlate with the prognosis of the patient or even severity of clinical manifestation (R. J. Martin, 2004; Menger & Jorg, 1999). Since lesions are usually located in vital areas, evidence of de- or even remyelination in vivo (i.e. biopsy) is almost impossible to get. So far, the studies done on the correlation of clinical outcome and radiologic neuroimaging failed to predict the severity and future recovery of cases analysed. This simple fact demonstrates the

problems researchers and clinicians are facing today and also illustrates the limitations of our study. It could, nevertheless, be demonstrated that sequential imaging is essential as a considerable subgroup of patients had a normal MRI initially but went on to develop recognizable lesions (Rebedew, 2016; Singh et al., 2014).

Recently, Haynes et al. presented a case of apparently longstanding subclinical CPM in a patient who was found to show evidence of remyelinating axons on autopsy (Haynes et al., 2018). Clinicians and researchers suspect a large number of unreported cases since not all patients become symptomatic. The condition has a highly variable prognosis and mortality appears to be much lower than initially thought, since with the advent of improved diagnostic methods it has been shown that most patients experience an acceptable outcome or even full recovery (Graff-Radford et al., 2011; Kallakatta et al., 2011; Menger & Jorg, 1999; Mochizuki et al., 2003).

Besides sensitive radiological methods, a promising future approach to early diagnosis could be the usage of a panel of sensitive biomarkers for oligo- and astrocyte death including, among others, GFAP, AQP4 or S100. These may be seen as an indicator for the viability of astrocytes and oligodendrocytes and thus an early indicator of their damage before apparent lesions form. These markers were positively correlated with neurological injury in the blood of ODS animal models (Bouchat et al., 2018; Gankam Kengne et al., 2011; Nicaise et al., 2019).

Concerning the management of CPM, it can generally be said that an active therapeutic approach has a positive impact on clinical outcome. Building on case reports and animal studies, reinduction of hyponatraemia, administration of urea, steroid therapy and/or plasmapheresis may have a significantly positive impact on prognosis

(Bhattarai et al., 2010; Bibl et al., 1999; Chang et al., 2014; Oya et al., 2001; Rebedew, 2016; Sanghvi et al., 2007). Also, targeted reduction of neuroinflammation via administration of infliximab (Iwama et al., 2011), minocycline (Gankam-Kengne et al., 2010), dexamethasone (Sugimura et al., 2005) or lovastatin (Takefuji et al., 2007) seem to have a positive influence on outcome in animal models of ODS.

1.4 Aetiology of Central Pontine Myelinolysis

Even though the exact pathomechanism behind ODS remains elusive, a common trigger of demyelination in clinical practice can often be traced back to an iatrogenic osmotic insult like rapid correction of chronic hyponatraemia, a mechanism which was demonstrated in clinical as well as in studies on other animals (Karp & Laureno, 1993; Laureno & Karp, 1997; Sterns et al., 1986; Wright et al., 1979). Multiple pathomechanisms have been proposed over the last decades. However, the most common predisposing factor for the pathogenic drive of glial damage remains electrolyte disturbance and especially hyponatraemia and its rapid correction in cells with reduced adaptive capacity. As already proposed in early descriptions of CPM, overly quick correction of hyponatraemia in the context of malnutrition, alcoholism, and critically ill patients remains the primary clinical reason for the development of CPM (Adams et al., 1959; Bouchat et al., 2018; Kleinschmidt-Demasters et al., 2006; Singh et al., 2014). A systematic review of studies on CPM conducted between 1964 and 2013 revealed a striking 50.5% of patients with ODS and concurrent alcoholism (Singh et al., 2014). Liver cirrhosis and malnutrition have been reported as second and third causes respectively. Tomlinson et al. first proposed the nowadays widely accepted theory of overly rapid correction of hyponatraemia in 1976 (Tomlinson et al., 1976). Later it was confirmed that induction of hyponatraemia and subsequent

rapid correction causes CPM-like lesions in rats (Kleinschmidt-DeMasters & Norenberg, 1981), dogs (Laureno, 1983), rabbits (Illowsky & Laureno, 1987) and recently in mice (Bouchat et al., 2018).

Current research postulates a multifactorial interplay of co-factors and predisposing conditions that lead to deficiencies in neuronal and glial energy supply and, therefore, to a lack of fuel for the ATPases in the brain (Ashrafian & Davey, 2001). This is supported by current literature as well as our clinical data on patients suffering from malnutrition, alcoholism and/ or liver disease and hypoglycaemia (Ashrafian & Davey, 2001; Bouchat et al., 2018; Iwama et al., 2011; Kleinschmidt-Demasters et al., 2006; Nicaise et al., 2019; Popescu et al., 2013), all of which leaves the patients and hence their cells in a malnourished, energy-deprived state predisposing them to the dramatic effects of osmotic insults. The most common predisposing factors leading to ODS have been summarized in Table 1.

Table 1: Factors predisposing to the development of ODS (Junker et al., 2020; Singh et al., 2014)

Alcoholism
Malnutrition (e.g., anorexia)
Liver cirrhosis
Liver transplant
Dialysis
Metabolic disorders
Selective Serotonin Reuptake Inhibitors (SSRI)
Diabetes
Primary/psychogenic polydipsia
Stem cell transplant

Severe burns
Hyperemesis (gravidarum)
HIV / AIDS

Another vital subgroup of CPM cases encompasses patients with liver transplants. This cohort seems to have the worst prognosis and the highest mortality rates. However, this patient group experiences mostly mild, if any, concurrent hyponatraemia and shows different clinical features (for example liver cirrhosis of other aetiology than alcoholism and demyelination restricted to the pons) distinct from the general group of CPM patients. It is yet to be determined if the worse clinical outcome is due to a higher susceptibility for or severity of pontine myelinolysis itself or to unfavourable comorbidities. These features, however, may allude to a different pathomechanism of CPM in that patient group (de Morais et al., 2009; Singh et al., 2014; Yu et al., 2004).

1.5 The brain, its adaptation to hyponatraemia and response to correction – pathophysiology of CPM

Changes in the osmolarity of interstitial fluids are constantly happening in the body. When the concentration of intracellular solutes is unaltered, water enters or leaves the cells crossing the semipermeable cell membrane to produce equal solute concentrations (osmosis). This leads, of course, to a shrinkage or swelling of the cells. The skull is a non-expandible compartment, therefore a tight homeostatic regulation is essential to maintain the volume and thus the physiological functions of the CNS (Nicaise et al., 2019). To prevent cell swelling or shrinkage, the brain parenchyma can respond to osmotic alterations by uptake or release of inorganic osmolytes

initially and, later, also organic osmolytes. In particular, astroglia play a prominent role in osmotic regulation in the brain. Specialized channels inside the cell membrane perform the uptake or release of ions or organic solutes. Although it is still under debate, demyelination in CPM seems to occur secondary to the loss of glial cells. Most likely, those glial cells undergo an adaptive process to hyponatraemic conditions. When low serum sodium levels are corrected too fast, those cells are unable to “turn off” the hyponatraemia-adapted program in time, finally leading to the death of those cells (see Fig. 1 for visualisation).

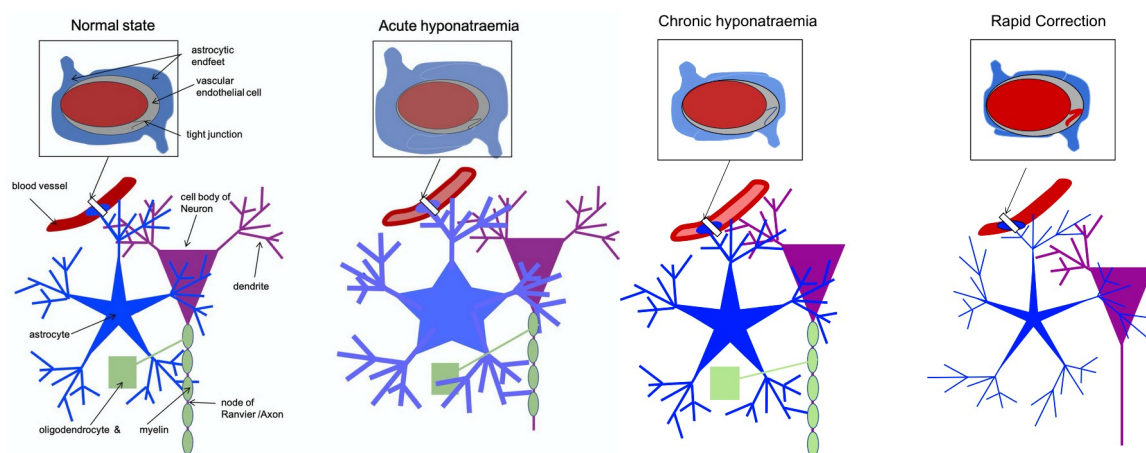


Fig. 1: Schematic representation of changes in the brain as response to osmotic stress. Normal state: osmotic balance between blood and the brain. Intact blood brain barrier with astrocytes wrapping blood vessels nearby. Acute hyponatraemia: water moves from blood into the brain causing cerebral edema to balance osmolality. Astrocytes undergo an adaptive process and release osmolytes. As water follows, brain cells shrink again. Chronic hyponatraemia: During prolonged hyponatraemia brain cells continue to lose inorganic as well as organic osmolytes to keep normal volume. As a consequence, osmolarity of brain cells is low -in balance with the dilute blood. Rapid correction: On rapid correction of hyponatraemia osmolality of the blood is quickly much higher than in the brain cells. Reuptake of osmolytes takes time. Thus, water flows from the brain into the blood to restore osmotic balance. The brain cells shrink and become dehydrated. As a result of this osmotic stress, astrocytes are damaged, oligodendrocytes and myelin are lost and the BBB gets disrupted. Adapted from Central Pontine Myelinolysis: A Metabolic Disorder of Myelin (Hurley et al., 2011)

Still, it is not known why some patients develop CPM on relative slow correction of sodium, while others will not go on to express CPM. This even holds true for conditions thought to serve as a “perfect” environment for the development of CPM like the enhancement of pathological drive via an extreme and rapid rise in sodium.

Besides hyponatraemia, hypokalaemia was found to be a trigger of CPM as well. It was hypothesised that hypokalaemic, as well as hyponatraemic conditions, increase the potential gradient against which the ATPase must pump (Bahr et al., 1990). This is particularly problematic as it increases the energy requirements of an already energy-deprived cell. Furthermore the ATPase pumps are necessary to maintain the tightly regulated electron gradient between extra- and intracellular compartments which is essential for the function of neurons. Without this gradient, neurons are not able to mount and propagate action potentials and are, therefore, unable to communicate with other cells and with each other.

Rapid and extreme electrolyte manipulation possibly on the background of previously deprived conditions (like alcoholism, malnutrition, etc.) with consequent increase of excitotoxic substances would thus lead to cellular water and nutrient loss, potentially triggering apoptosis and demyelination. This is thought to happen due to increased permeability of mitochondria in response to metabolic stresses as well as increased production of free radicals and intracellular increase in calcium (Ashrafian & Davey, 2001; Banerjee, 2014; Garland & Halestrap, 1997). Besides, it has been proposed that an increased level of inducible nitric oxide synthase (iNOS) which is well recognized in patients with a history of alcohol abuse, aggravates the cytotoxic/apoptotic environment for glia and myelin (Lancaster, 1995; Leist & Nicotera, 1998). Moreover iNOS can, by itself, lead to an increased production of free radicals which further drives apoptosis and destruction cells (Stadler et al., 2008).

The tendency of CPM to develop in the human pons and midbrain is likely due to the unique arrangement of axons and neurons forming a tight grid in and close to the pons. The small vessels in the central pons show a low perfusion pressure and the

grid arrangement lead to steric restrictions that limit the ability of the cells to adapt (for instance by swelling) in response to electrolyte derangement. Their only option is to lose ions to adapt to electrolyte derangement which leaves the cells even more at risk of damage upon osmotic stress. These facts, the tight arrangement and the low perfusion pressure within the pons, might be the two main factors responsible for the predilection of ODS to the central pons (Ashrafian & Davey, 2001; Hurley et al., 2011; Riggs & Schochet, 1989; Wedeen et al., 2012).

However, even if the hypotheses proposed seem to explain a great part of why CPM develops, preferably in chronic alcoholics, there are multiple inexplicabilities with it and they are only partly supported by clinical data.

CPM is a very heterogeneous disorder and most patients who experience correction of hyponatraemia do not suffer any symptoms. It might be worth a thought if the aetiology of hyponatraemia may play a role in the development of CPM, like some studies suggest (Ashrafian & Davey, 2001).

1.6 Pathology of myelin

Myelin acts as insulation around axons to ensure high-speed electrical signal conduction. Myelin sheaths are made by mature oligodendrocytes that arise from oligodendrocyte precursor cells and neural stem cells (Goldman & Kuypers, 2015; Zuchero & Barres, 2015). Myelin consists of membrane lipids and myelin proteins. Of these myelin proteins, PLP is the most abundant in the CNS, whereas MBP is the only myelin protein known to be essential for myelin assembly (Weil et al., 2016). Besides PLP and MBP, the glycoproteins MAG and MOG can be found and are regularly used for myelin-specific immunohistochemical (IHC) staining. In adults,

mature oligodendrocytes serve the primary goal of nurturing and preserving the established myelin sheaths (Boullerne, 2016; Goldman & Kuypers, 2015). Primary myelin or oligodendrocyte pathologies, as it is the case in ODS, consequently result in disturbances in the electrical conduction of axons. However, axons and neuronal cell bodies are relatively preserved (Adams et al., 1959; Nicaise et al., 2019). Some approaches focus on the role of apoptosis of oligodendrocytes in osmotic demyelination. Ashrafian et al., for example, as well as DeLuca et al. found a convincing link to apoptotic pathways which are known to be the preferred mechanism of oligodendrocyte death (Ashrafian & Davey, 2001; DeLuca et al., 2002).

Besides myelin and oligodendrocytes, astrocytes are also affected in ODS. Based on animal studies it has been proposed that, mechanistically, the osmotic insult leads to astrocytopathy and is followed by oligodendrocytopathy and finally demyelination (Bouchat et al., 2018; Gankam Kengne et al., 2011; Gankam-Kengne et al., 2017; Illowsky & Laureno, 1987; Kleinschmidt-DeMasters & Norenberg, 1981; Laureno, 1983). Whether a similar sequence of events also occurs in CPM is still unclear, since clinical and post-mortem studies on human patients are still relatively sparse (Gocht & Colmant, 1987; Gocht & Lohler, 1990; Rao et al., 2015).

1.6.1 Astrocytopathy and oligodendrocytopathy

Animal models of ODS shed more light on the crucial role of astrocyte (dys-)function in demyelinating diseases and oligodendrocyte pathology. Astrocytes play a crucial role in regulating water and ion exchange at the gliovascular interface, via AQP1 and AQP4 and the proximity of foot processes to the brain's vasculature. It has been shown that not only oligodendrocytes but primarily astrocytes suffer from osmotic

stress and might trigger the cascade of ODS (Bouchat et al., 2018; Gankam Kengne et al., 2011; Nicaise et al., 2019). Moreover, Iwama et al. reported the secretion of proinflammatory cytokines by astrocytes and microglia which serve as possible triggers of oligodendrocyte and thus myelin loss. This hypothesis is further supported by studies demonstrating reduced demyelination and symptoms upon interventions that inhibit microglia activation, suggesting that the signaling cascades initiated by astrocyte pathology and potentiated by microglia activation, might represent the initial event in ODS (Iwama et al., 2011; Moore et al., 2011; Nicaise et al., 2019; Takefuji et al., 2007).

Myelination, which necessitates recruitment and proliferation as well as differentiation and maturation of oligodendrocytes, relies on communication between astrocytes and oligodendrocytes, either by direct cell-cell contact or by factors secreted by astrocytes (Domingues et al., 2016).

Electric as well as metabolic coupling via gap junctions and their close contact build the basis of this essential glial crosstalk (Dutta et al., 2018; Iacobas & Iacobas, 2010; Menichella et al., 2003). The connection is necessary as astrocytes aid in multiple aspects of myelination, spanning removal of debris to the structural support of myelin and involvement in oligodendrocyte precursor cell migration and proliferation. Magnotti et al. demonstrated lethal consequences of a disturbed crosstalk between oligodendrocytes and astrocytes, via genetically modified mice with double knockout of oligodendrocyte and astrocyte connexins (Magnotti et al., 2011). Animal models on experimental ODS, have demonstrated loss of oligodendrocyte and astrocyte connexins in ODS. Besides loss of connexins, loss of other astrocytic proteins, like GFAP, AQP1 and AQP4 and S100b, have been demonstrated. The same team later

showed that apoptosis of astrocytes as well as loss of oligodendrocytes occurs early in lesion development and most importantly before loss of myelin proteins was apparent. Moreover, astrocyte apoptosis was restricted to areas of future demyelination (Gankam Kengne et al., 2011; Gankam-Kengne et al., 2017).

However, the exact mechanisms of astrocytes and oligodendrocyte demise, the local regulatory factors and the induction of regeneration and remyelination remain largely unexplored. Nevertheless, based current research on (inflammatory) demyelinating diseases, general pathological changes in human CPM can be inferred:

1. Early production of pro-inflammatory cytokines by astrocytes and activated microglia (Choi et al., 2014; Iwama et al., 2011; Rawji et al., 2020)
2. Dysregulation of AQP and GFAP expression (Mader & Brimberg, 2019; Popescu et al., 2013, p. 4)
3. Disturbance and loss of gap junctions and connexins (Li et al., 2014; Lutz et al., 2009; Menichella et al., 2003)
4. Rise in apoptotic cell markers (Bax, Bak, Bim, death receptor 3) (DeLuca et al., 2002)
5. Astrocytopathy and relative preservation of oligodendrocytes (Bouchat et al., 2018; Gankam Kengne et al., 2011; Hurley et al., 2011; Lohrberg et al., 2020; Nicaise et al., 2019; Singh et al., 2014)
6. Increased reactivity (ramification & branching) and delayed loss of oligodendrocytes (Bouchat et al., 2018; Gankam Kengne et al., 2011; Hurley et al., 2011; Nicaise et al., 2019; Singh et al., 2014)

7. Myelin swelling and damage (Hurley et al., 2011; Singh et al., 2014)
8. Transient opening of the BBB (Bouchat et al., 2018)

1.7 Aims of the study

Using animal models of ODS, it is possible to determine the time course of de- and remyelination. Nevertheless, the translation from animal models to patients is challenging. In this study, we histologically investigated a cohort of human CPM patients to establish a plausible time course of CPM/ODS disease pathology with a focus on astrocyte and oligodendrocyte dynamics.

2 Material und Methods

2.1 Patient tissue

We retrospectively searched the database of the Institute of Neuropathology of the Universitätsmedizin Göttingen (UMG) for post-mortem autopsy brain tissue of patients diagnosed with CPM, including the patient cohort of Prof. Andreas Gocht. A cohort of 15 males and five females with sufficient tissue available for further analysis were included in the present study with an average age of 54.3 years (Table 4).

The dissertation at hand forms part of a larger study conducted at the Institutes of Neuropathology of the UMG and the Universitätsklinikum Leipzig in collaboration with the Neuropathology department at Klinikum Kassel. The study was approved by the ethics committee of the UMG. Clinical and histopathological information on seven cases was previously published (Gocht & Colmant, 1987).

2.2 Histology and immunohistochemistry

2.2.1 Basic concepts

To take micrometre-thin cuts from fixed tissue, it must undergo a systematic embedding process. The principle of the embedding process involves replacing the tissue fluid by a subsequent one, namely the embedding medium which is solid at room temperature (usually paraffin wax). For embedding, the wax is liquefied by heating. Through various intermediate steps, the embedding medium penetrates the tissue network and solidifies during cooling. The tissue sample is placed into a mold,

covered with embedding medium and allowed to harden. This process is called “blocking.”

Table 2: Embedding protocol – Excelsior AS1 & AS2 (Einbettungsprozess des Instituts für Neuropathologie, Universitätsmedizin Göttingen, valid since last revision on 26th Feb, 2019)

			AS2	AS1
			Biopsies	Autopsies
	Step	Reagent	Incubation time	Incubation time
Dehydration Isopropanol	Fix 1	50% Isop	30 min	2 h
	Fix 2	50% Isop	30 min	2 h
	I 1	70% Isop	1 h	3 h
	I 2	90% Isop	1 h	3 h
	I 3	96% Isop	1 h	3 h
	I 4	100% Isop	1 h 30 min	3 h
	I 5	100% Isop	1 h 30 min	4 h
Xylol	I 6	100% Isop	1 h 30 min	4 h
	X 1	Xylol	1 h 15 min	2 h
	X 2	Xylol	1 h 15 min	2 h
Paraffin	X 3	Xylol / 45°C	1 h 15 min	2 h
	W 1	Paraffin / 63°C	1 h 15 min	2 h
	W 2	Paraffin / 63°C	1 h 15 min	2 h
	W 3	Paraffin / 63°C	1 h 15 min	2 h
Duration			16 h 08 min	36 h 28 min

1 μm thick sections were obtained from the tissue blocks using a microtome and placed onto silanized microscope slides. Prior to staining, the slices were placed in an incubator at 58°C for 10 minutes to melt the paraffin and subsequently soaked in xylene three times for 4 minutes and once in iso-xylene for 4 minutes for deparaffinization. Then sections were rehydrated in 100% alcohol twice for 3 minutes followed by a stepwise series of diluted alcohol in 90%, 70% and 50% alcohol for 2 minutes each. For completion of the rehydration process, the sections were placed in distilled water for 2 minutes.

2.2.2 Hematoxylin and Eosin (HE)

Haematoxylin and Eosin (HE) staining allows for visualization of the basophilic structures like cell nuclei and their DNA as well as ribosomes which would stain blue on haematoxylin. Acidophilic structures like plasma proteins of the cells stain red on Eosin. The first step for haematoxylin staining comprises an 8-minutes bath of the deparaffinized sections in Mayer's haematoxylin. Followed by a brief rinse of the slides in distilled water and subsequently in HCl-ethanol for differentiation. To increase the pH and hence to enhance the blue colorization of the tissue, the samples were then carefully rinsed under running tap water for 10 minutes. Following haematoxylin staining, the sections were bathed in Eosin for 5 minutes and subsequently again rinsed with distilled water for 2 minutes.

To finish the H&E staining process, the sections underwent dehydration by moving the sections through a series of 50%, 70%, and 90% of diluted ethanol for 2 minutes each. The slides were then bathed in 100% ethanol two times for 3 minutes, followed again by a bath in iso-xylene for 4 minutes. Then, the slides were rinsed three times

with xylene for 4 minutes each. Finally, the now stained sections were mounted with DePex and dried at room temperature before considered ready for analysis under the light microscope.

2.2.3 Luxol Fast Blue/ Periodic Acid Schiff stain

Luxol-Fast Blue staining allows for visualization of the myelin sheaths on formalin-fixed, paraffin-embedded sections. Myelin and phospholipids stain blue-green, whereas the grey matter and demyelinated areas appear pink. This stain is routinely used to identify the basic neuronal and myelin structure in brain or spinal cord tissue. For this procedure, the sections again have to be deparaffinized and rehydrated (compare H&E staining protocol). This step, however, is then followed by a bath in a Luxol fast blue solution at 60°C overnight. The sections were then cooled and rinsed in 90% ethanol to remove any excess stain. For further differentiation, the slides were then pulled through a 0.05% lithium carbonate solution, 70% ethyl alcohol for 30 seconds in turn and washed in distilled water. For the second staining procedure, the Periodic Acid Schiff (PAS) reaction, the sections were incubated in 1% Periodic Acid for 5 minutes, rinsed under running tap water again for 5 minutes and then rinsed thoroughly in distilled water. The slides remained in the Schiff reagent for 20 minutes and were then washed under tap water for 5 minutes. This step establishes the bluish colorization of the nuclei. Finally, the slides were successively bathed in 1% HCl alcohol, rinsed with tap water and moved through an ascending alcohol series to be placed in xylene. In the end, the slides were mounted with DePex and dried at room temperature.

2.2.4 Immunohistochemistry. Application and Protocol

Immunohistochemistry (IHC) is a standard method of immunostaining and encompasses an antibody-based method to detect a specific protein of interest in a sample of human tissue. IHC can utilize monoclonal as well as polyclonal antibodies to identify the distribution of the antigen of interest. The procedure dates back to Albert Coons in 1941 and has two possible protocols to be followed (Coons et al., 1941; Ramos-Vara, 2005).

Direct immunohistochemistry

Direct IHC is the quicker method in which one labeled antibody directly binds to its target antigen. This technique utilizes only one antibody. While the procedure is fast, it is less sensitive due to little signal amplification. Therefore, it is rarely used nowadays.

Indirect immunohistochemistry

The indirect method is the advanced form of IHC and involves multiple layers of antibodies. During the first incubation step, an unlabeled primary antibody binds to the tissue antigen. The secondary antibody is detecting the constant region of the primary antibody and is labelled linked to either an enzyme or a fluorophore, enabling detection. Important to note is that the secondary antibody has to be directed against the IgG of the animal species (e.g. mouse or rabbit) in which the primary antibody has been produced. As several secondary antibodies can bind to different antigenic sites of the primary antibody there is a signal amplification. Therefore, the indirect method is much more sensitive compared to the direct IHC.

Table 3: Antibodies used for IHC and/or immunofluorescence

Antibody	Species	Dilution	Clone	Manufacturer
Anti-AQP4	Rabbit	1:100	Polyclonal	Merck, Millipore
Anti-GFAP	Rabbit	1:1000	Polyclonal	Dako
KiM1P	Mouse	1:5000	Cell culture supernatant	Neuropathology, UMG; clone kindly provided by Prof. Radzun, Institute of Pathology, UMG
Anti-Iba1	Mouse	1:100	Polyclonal	Merck, Millipore
Anti-Ki67	Rabbit	1:200	Polyclonal	DCS
Anti-MAG	Mouse	1:500	EP971Y	Abcam
Anti-MBP	Rabbit	1:500	Polyclonal	Dako
Anti-MOG	Rabbit	1:500	EP4281	Abcam
Anti-PLP	Mouse	1:250	plpc1	Biorad, BZL04478
Anti-p25	Mouse	1:1000	6C10	gift from Prof. Timea Berki, Pécs, Hungary

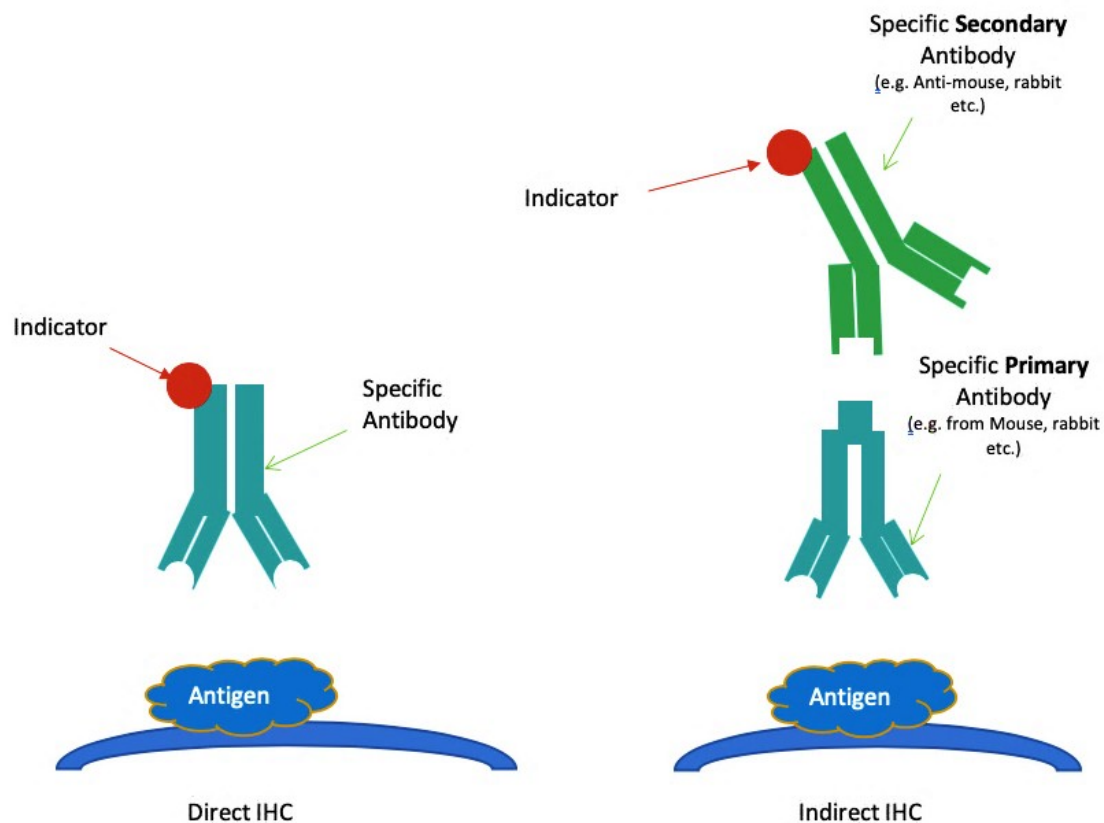


Fig. 2: Principle of IHC direct versus indirect method. Adapted from Principles of IHC staining ('Principles of IHC staining | Cell Signaling Technology', n.d.).

Protocol

Following the deparaffinization and rehydration, as described earlier, the samples were treated with antigen retrieval reagents to loosen any crosslinks between proteins due to tissue fixation and hence enable the primary antibody to reach its designated target protein. These antigen retrieval agents differ depending on the primary antibody applied (either Citrate or EDTA buffer, 3 times 5 min microwave).

To visualize the protein of interest, peroxidases are used. Therefore, endogenous peroxidases have to be blocked beforehand, as to prevent false-positive results. To do so, the samples were bathed in 3% hydrogen peroxide in PBS for 1h at room temperature. This was, again, followed by a thorough wash out in distilled water and PBS.

The slides were incubated in 10% fetal calf serum (FCS) diluted in PBS for about 30 minutes at room temperature to prevent the unspecific binding of the antibodies. The primary antibody was diluted in 10% FCS, applied to each sample and allowed to bind in a humidity chamber at 4°C, overnight. Next, the slides were washed with PBS four times. The secondary antibody was diluted in 10% FCS and applied to each sample. The slides were then incubated in a humidity chamber at room temperature for one hour and following that, thoroughly washed in PBS. Subsequently, the slides were put into a DAB solution (25 mg of 3,3-diaminobenzidine (DAB) and 20 µL of 30% hydrogen peroxide diluted in 50 ml of PBS). The enzymatic reaction with peroxidase coupled to the secondary antibody leads to brown colouring. DAB reaction was kept under visual control to avoid overstaining. The slides were then washed under distilled water. The slides were very briefly treated with Mayer's Hematoxylin for counterstaining of the nuclei and again washed with distilled water. This was followed by a quick rinse in 1% hydrochloric acid alcohol for differentiation and a thorough wash under running tap water for 10 minutes. The slides were then dehydrated again via a wash in distilled water, moving the slides subsequently through 50%, 70%, 90% and 100% alcohol for 3 minutes and a bath in xylene for 5 minutes for dehydration. Lastly, the now stained slides were mounted with DePex and dried at room temperature.

2.3 Implementation

Extent and localization of demyelination was first determined by staining with LFB. We then looked at the myelin proteins: proteolipid protein (PLP), myelin oligodendrocyte glycoprotein (MOG), Myelin-associated glycoprotein (MAG) and myelin basic protein (MBP) and determined their absence or if they were present

again. We further analyzed astrocytic markers (aquaporin 4, AQP4; glial fibrillary acidic protein, GFAP), oligodendroglial markers (p25), markers for macrophages/activated microglial cells (KiM1P) and Ionized calcium-binding adaptor molecule 1 (Iba1) as a microglial and monocyte-specific protein which stains all microglia, “resting,” activated as well as infiltrating monocytes. Cellular proliferation was estimated by Ki67 immunoreactivity.

2.4 Estimation of demyelination

The presence of the myelin proteins was estimated by a semi-quantitative scoring system consisting of low, medium or high abundance of immunoreactivity for MBP, MAG, MOG or PLP.

2.5 Analysis of cell density and proliferation

The extent of astrocyte or oligodendrocyte loss, as well as macrophage invasion in CPM lesions, was quantified manually using light microscopes and standardized counting grids within and outside lesion areas. To quantify cells within the lesion border, half of the counting grid was placed inside and half outside the lesion. Proliferating cells were double-stained with a combination of Ki67 and the suitable cell type marker.

2.6 Data plotting and statistical analysis

Data plotting and statistical analysis was performed using Graph Pad Prism Version 8. To compare the means of cell densities between lesion, border and perilesional areas, we utilized paired t-tests for comparison of two groups or one-way ANOVA with post-hoc tests for more than three groups. Unless otherwise stated,

data points represent mean values and bars or lines represent group means \pm standard error of the mean. The significance level was set to be $p < 0.05$.

3 Results

3.1 Patient cohort

We were interested in the mechanisms of lesion formation and repair in our cohort of patients suffering from CPM. We began by examining pontine lesions in post-mortem material of 20 CPM patients. Clinical information on cause of death was available for 18 cases, information about development of coma for 20, history of alcohol abuse for 20 and records of time since onset of symptoms was found for 6 cases (see Table 4). Of the 20 patients, 15 were male (75%), and 16 (80%) had a history of alcohol abuse. The majority of the cohort, nine patients (45%), died from cardiovascular failure, six patients (30%) due to pneumonia or respiratory failure, two succumbed to multiple organ failure and one died from liver failure.

Table 4: Clinical information on CPM patients

Subject	Age	Sex	Symptom onset (d)	Coma	Alcohol abuse	Cause of death
1	46	m	48	no	yes	na
2	40	f	20	no	yes	Cardiovascular failure
3	63	m	15	no	yes	Cardiovascular failure
4	41	m	20	no	yes	Pneumonia
5	50	m	na	yes	no	Cardiovascular failure
6	38	m	11	yes	yes	Pneumonia
7	58	m	na	no	yes	Cardiovascular failure
8	57	m	na	no	yes	Multiple organ failure
9	32	f	na	no	yes	Respiratory insufficiency
10	24	m	na	no	no	Multiple organ failure
11	43	f	na	yes	yes	Pneumonia
12	50	m	na	no	no	Cardiovascular failure
13	46	f	na	no	yes	na
14	36	f	na	no	yes	Cardiovascular failure
15	47	m	na	no	yes	Respiratory insufficiency
16	50	m	na	no	yes	Pneumonia
17	80	m	na	no	yes	Cardiovascular failure
18	15	m	na	no	no	Liver failure
19	63	m	15	no	yes	Cardiovascular failure
20	67	m	4	yes	yes	Cardiovascular failure

na: not available, d: Days between symptom onset and death; m: male, f: female; †: History of alcoholism

Table 5: Characteristics of patients with CPM

Variable	Number of cases (n=18)
Age (median in years)	48.5, ranging from 15 -80 years
Sex (male:female ratio)	75%
Coma	18%
Alcohol abuse	80%
Liver cirrhosis	6.3%
HIV	12.6% (rest na)
Cardiovascular pathology	45%

3.2 Characteristics of demyelination

By LFB/PAS staining we found singular or, more rarely, multiple demyelinated lesions in the pons in all cases.

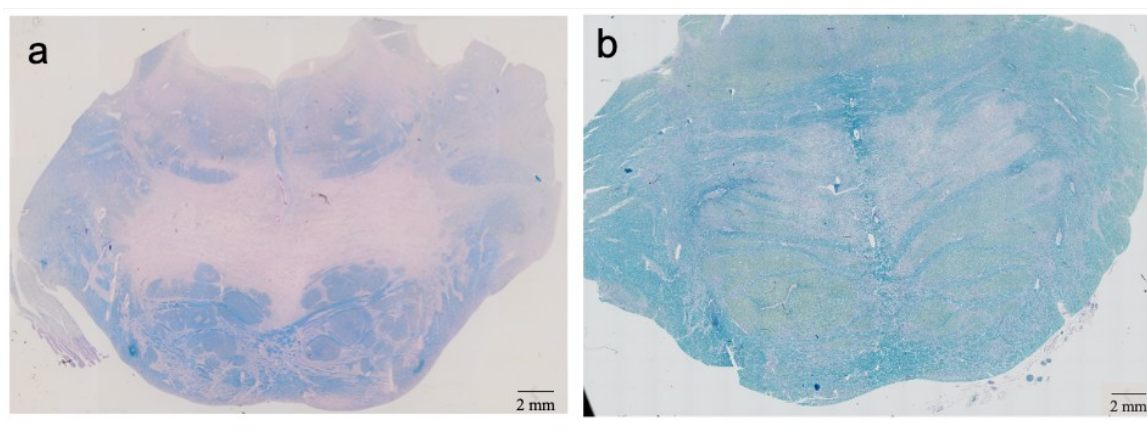


Fig. 3: Representative microphotographs of CPM lesions visualized by LFB/PAS staining. **a** Light microscopic image of the pons from an early-stage CPM patient showing sharply demarcated, bat-shaped myelin loss (patient no 14). **b** Light microscopic image of

the pons of a late-stage human CPM patient showing remyelination over the whole basis pontis without clearly demarked lesions (patient no 16) ; 40x magnification; scale bar represents 2mm.

The majority (n=15) of lesions showed sharply demarkated lesions with clear boundaries and confluent demyelination as illustrated above (Figure 3a). On the other hand, five cases showed a more varied picture with irregular expression of myelin, less sharply demarkated borders or even remyelination as depicted in Figure 3b; (n=5).

We wanted to assess whether the loss of myelin, as indicated by loss of LFB staining, was accompanied by loss of myelin proteins and applied a semi-quantitative scoring system. Unsurprisingly, we found predominantly low or absent myelin proteins within human CPM lesions. We performed in depth disease staging by evaluating further cellular marker proteins: MBP (myelin), GFAP (astrocytes) and Kim1P (macrophages/activated microglia).

3.3 CPM lesion and disease staging

To determine the presumed stage of lesion development in our patients, we analysed the presence and appearance of myelin, the presence of macrophages/activated microglia as well as phagocytosis and the astrocyte density and morphology. We paid particular attention to bipolar and/or reactive astrocytes, as well as their AQP4 immunoreactivity. We excluded two cases from indepth histological analysis due to extensive gliosis. We divided the rest of the cohort into early (n=5), intermediate (n=5) and late (n=8) disease stages. Figures 4-6 depict representative cases of each lesion stage.

The **early stage** of CPM lesion formation is characterized by a complete loss of myelin in LFB staining and IHC for myelin proteins (e.g. MBP). Further, a massive infiltration of KiM1P positive macrophages/activated microglial cells was seen. Astrocytes were substantially decreased in the lesions; astrocytes with bipolar morphology were observed and were frequently AQP4-negative. Reactive astrocytes were found predominantly at the lesion border, whereas in later lesion stages, they were also found closer to the lesion center. Some clasmatodendrosis, i.e. an “irreversible degenerative change with extensive swelling and vacuolization of cell bodies and disintegrated processes” (Ryu et al., 2011) was seen as a sign of astrocyte damage. In some cases, phagocytosis of myelin by macrophages was observed (compare Fig. 18).

The **intermediate stage** lesions showed myelin loss and numerous infiltrated KiM1P-positive macrophages/activated microglia inside the lesion area. In contrast to the early stage, astrocyte densities appeared increased (even compared to the

perilesion) and astrocyte morphology was more ramified and often bipolar, indicating repopulation of the lesion area. Also, in most lesion areas, astrocytes showed a polarized expression of AQP4.

The ***late-stage*** lesions still showed KiM1P-positive cells within the lesion, which were, however, less dense and often showed a more ramified morphology. Lesions were partly remyelinated as indicated by pale LFB staining, and astrocyte densities were comparable to perilesional areas, positive for AQP4 and seemed to be of a denser, round morphology with fewer ramifications.

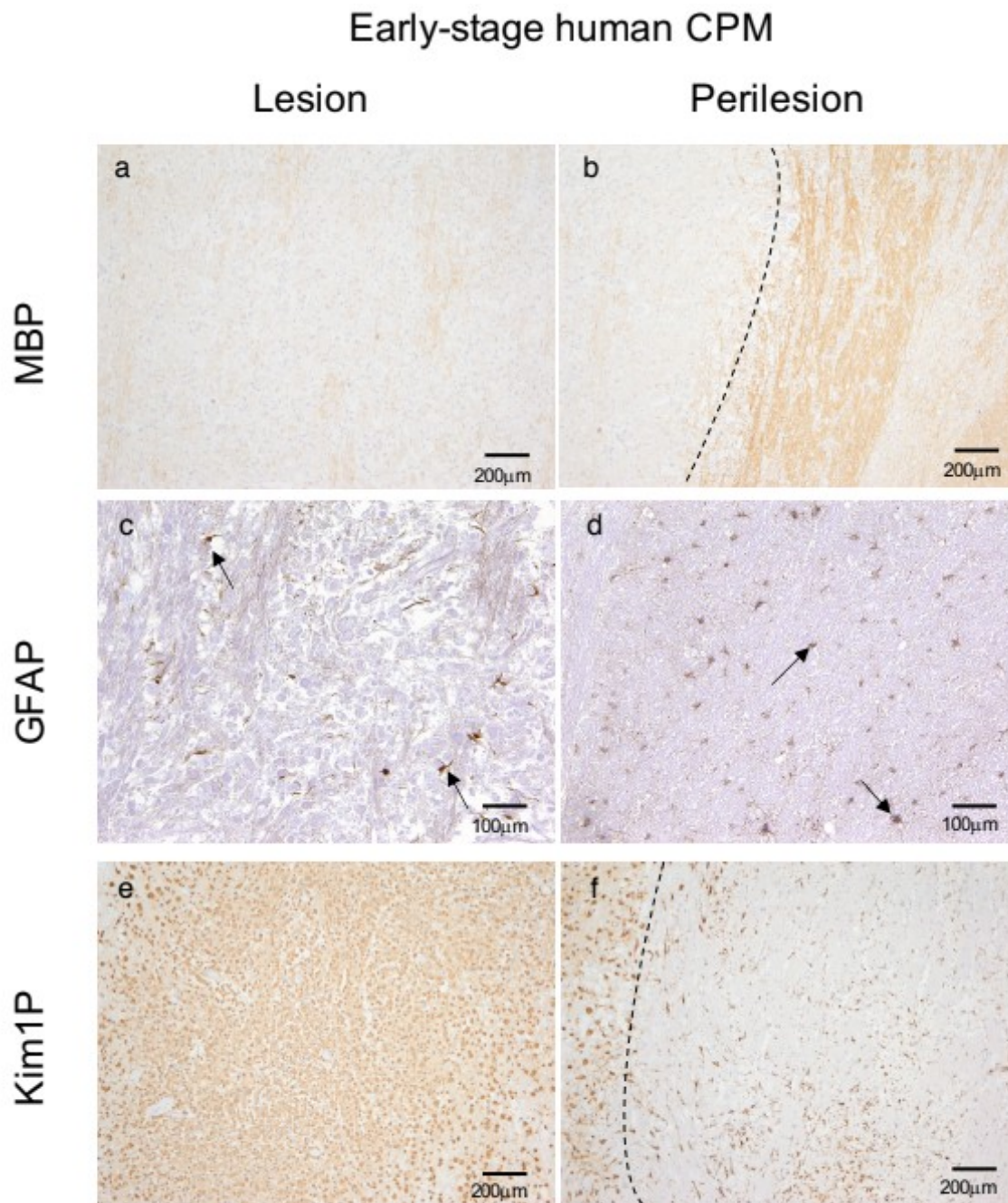


Fig. 4: Features of early-stage CPM. Patient no 9. **a-b** Myelin basic protein (MBP) depicting the demyelinated lesion area (**a**) and preserved myelin in the periplaque area (**b**). The dashed line marks the border between lesion on the left and perilesion on the right side. 40x magnification, scale bar represents 200 μ m. **c-d** IHC of the astrocytic intermediate filament GFAP, depicting loss of astrocytes within the lesion area (**c**) compared to the perilesion area (**d**). 100x magnification, scale bar represents 100 μ m. **e-f** Immunohistochemical staining against Kim1P, marking activated foamy macrophages/activated microglia in the lesion area (**e**), but few in the perilesion area (**f**). The dashed line marks the border between lesion on the left and perilesion on the right side. 40x magnification, scale bar represents 200 μ m.

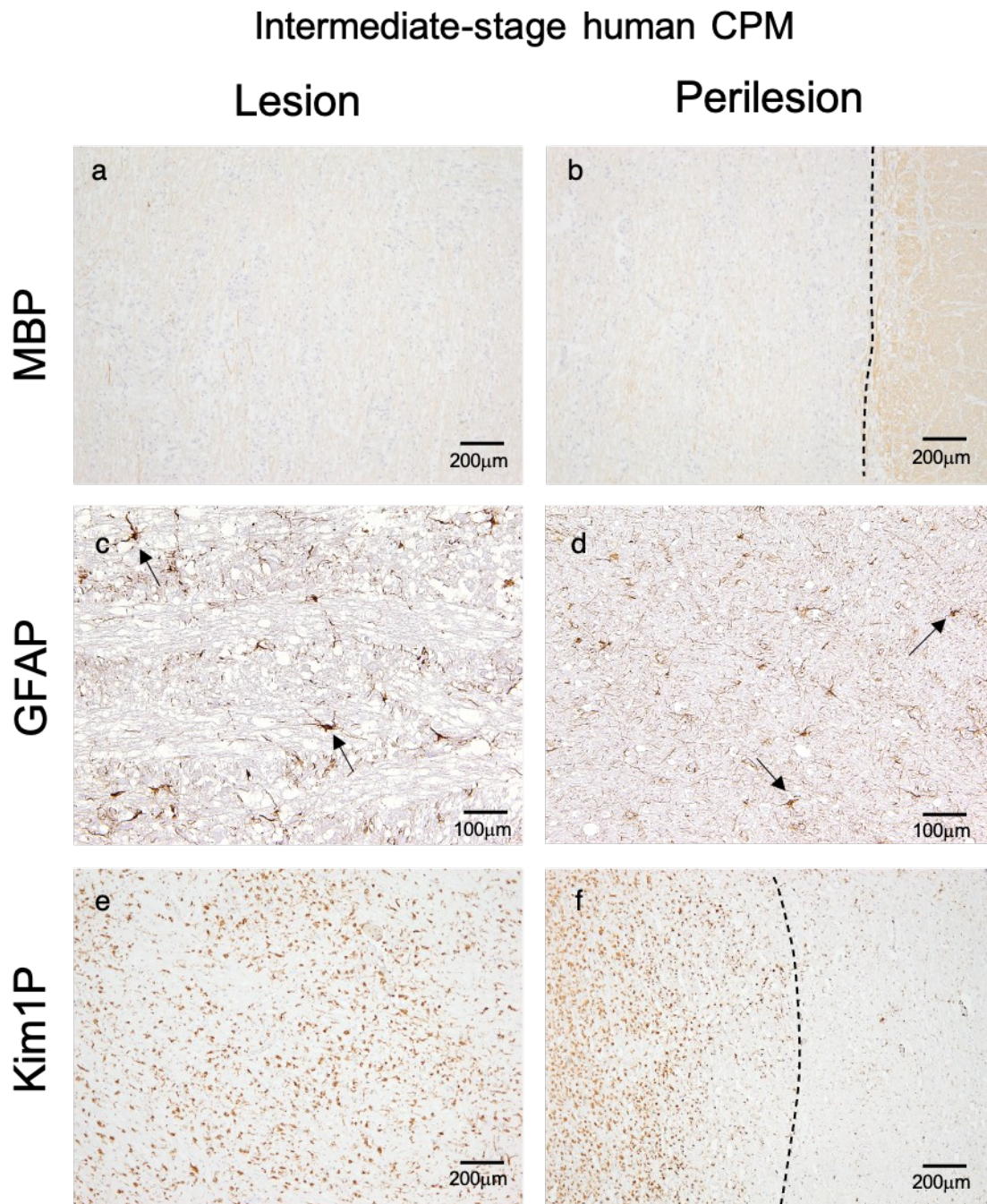


Fig. 5: Features of intermediate-stage CPM. Patient no 15. a-b IHC against myelin basic protein (MBP) depicting the demyelinated lesion area (**a**) and preserved myelin in the periplaque area (**b**). The dashed line marks the border between lesion on the left and perilesion on the right side. 40x magnification, scale bar represents 200µm. **c-d** IHC of the astrocytic intermediate filament GFAP, depicting a reduced density of astrocytes within the lesion area (**c**) compared to the perilesion area (**d**). 100x magnification, scale bar represents 100µm. **e-f** IHC against Kim1P, marking substantial macrophages and activated microglial cells in the lesion (**e**), and few in the perilesion area (**f**). The dashed line marks the border between lesion on the left and perilesion on the right side. 40x magnification, scale bar represents 200µm.

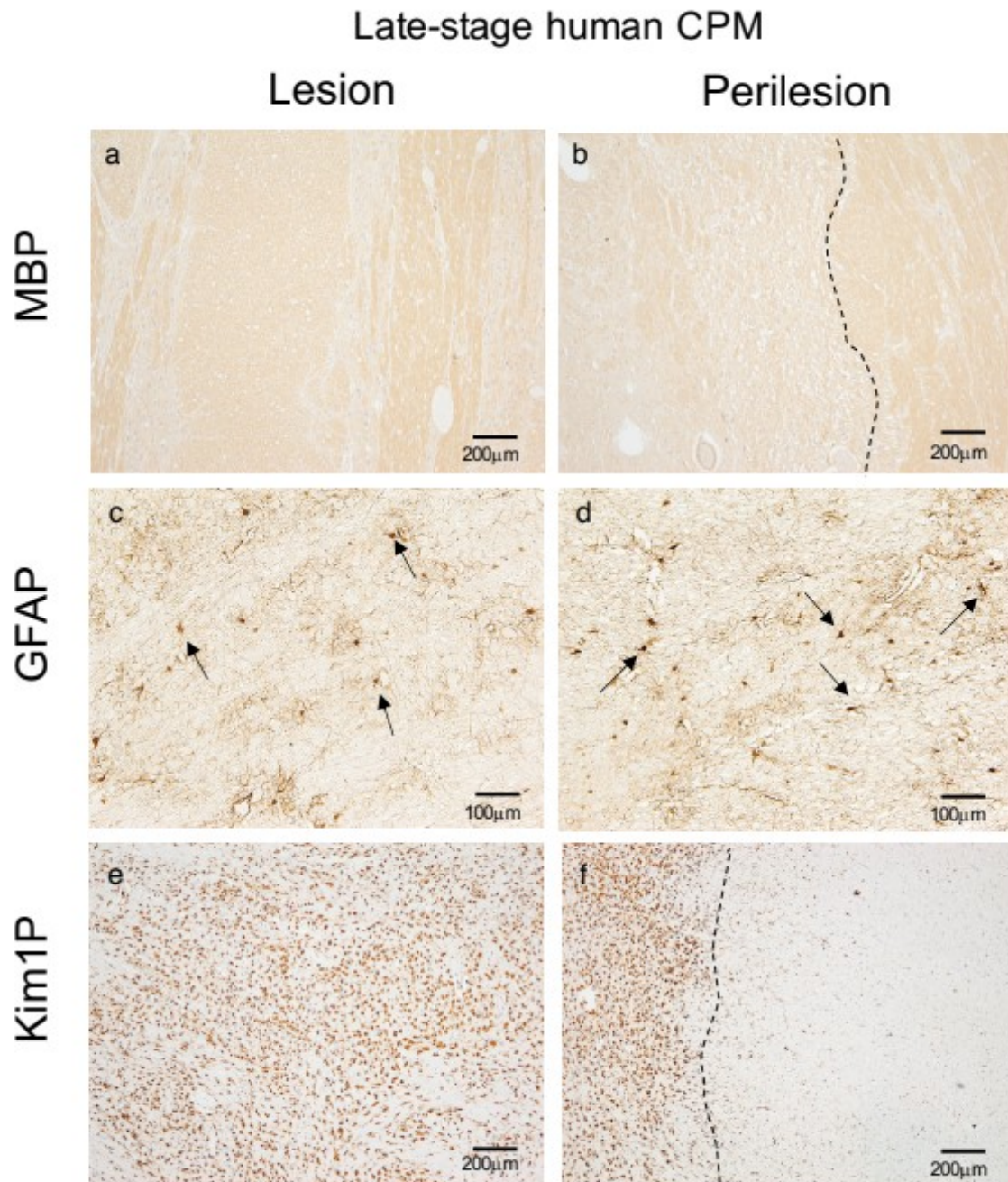


Fig. 6: Features of late-stage CPM. Patient no 3. **a-b** IHC against myelin basic protein (MBP), depicting a largely remyelinated lesion centre (**a**) and the border between lesion and perilesion (**b**). The dashed line marks the border between lesion on the left and perilesion on the right side. 40x magnification, scale bar represents 200 μ m. **c-d** IHC of the astrocytic intermediate filament GFAP, depicting reactive astrocytes within the lesion area (**c**) compared to the perilesion area (**d**). 100x magnification, scale bar represents 100 μ m. **e-f** IHC against Kim1P, marking macrophages/activated microglial cells in the lesion area (**e**), but not in the perilesion area (**f**). The dashed line marks the border between lesion on the left and perilesion on the right side. 40x magnification, scale bar represents 200 μ m.

3.4 Astrocytes within human CPM lesions

3.4.1 Astrocyte densities are decreased in early CPM lesions

As shown in experimental models, astrocyte loss is thought to be an early event in ODS lesions (Gankam Kengne et al., 2011). However, CPM/EPM lesions are characterized by variable astrocyte density in the literature (ADAMS et al., 1959; Gocht & Colmant, 1987; Popescu et al., 2013), indicating the need for lesion staging to explain this variability. We quantified the density of astrocytes within the de-/partly remyelinated lesions, at the lesion border and in myelinated perilesional areas using double labelling of LFB-PAS- and GFAP-IHC. The early human CPM cohort (n=5) showed significantly less astrocytes in the lesion center, compared to the periplaque area with the highest mean density of astrocytes per mm² (Lesion: 72.0±25.3; Perilesion: 160.0±33.9; paired t-test; p=0,0303). The intermediate- and late-stage CPM subgroup did not show significant differences in astrocyte density between lesion center or perilesional area (intermediate-stage lesion: 156.2±34.94; perilesion: 150.4±24.1; paired t-test; p=0,8698 and late-stage lesion: 102±22.2; perilesion: 114.0±11.5; paired t-test; p=0,7097).

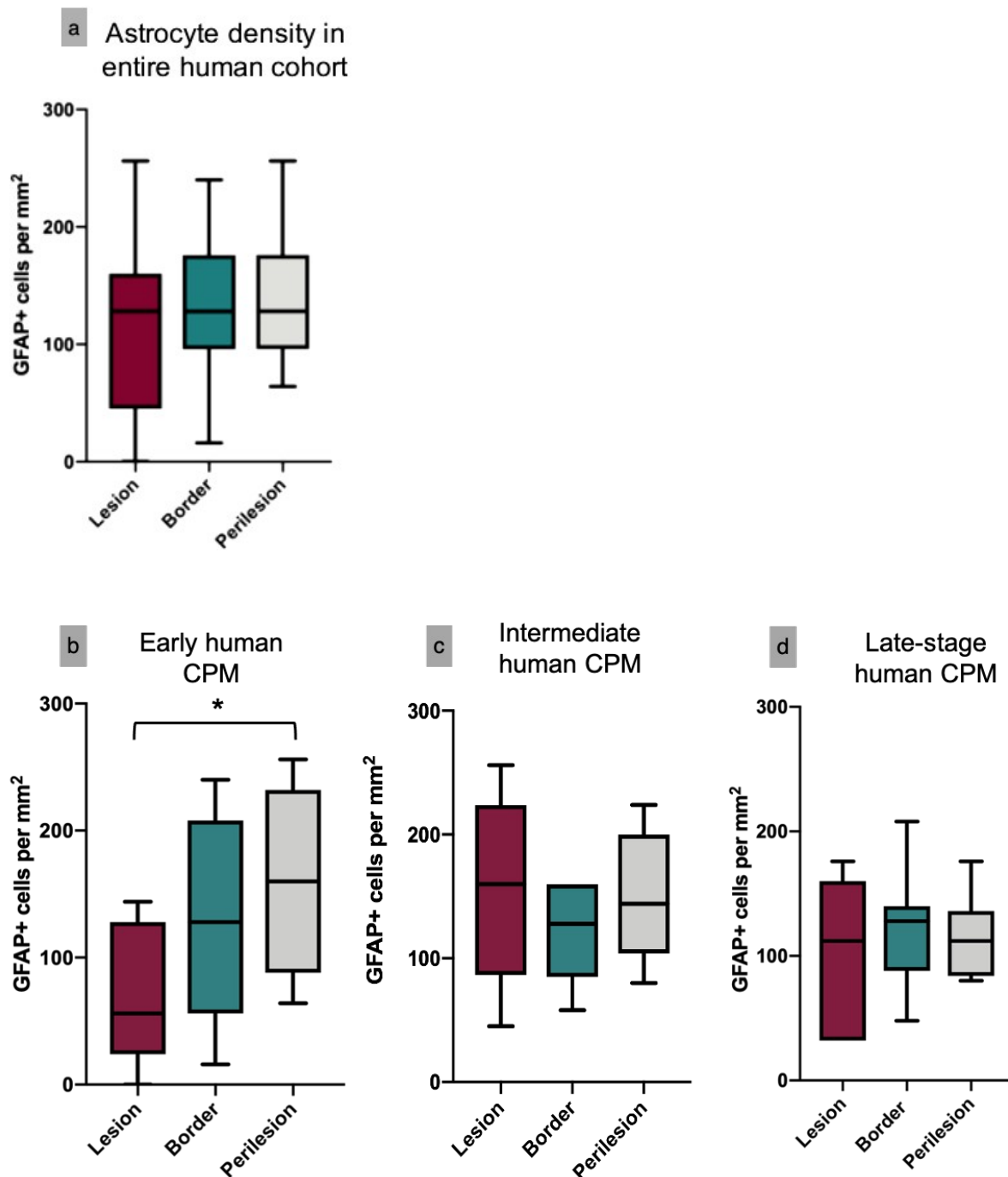


Fig. 7: Astrocyte density in early-, mid-stage and late-stage human CPM. **a** Astrocyte density in lesion centre, border and perilesional area showing no significant difference over the whole cohort. **b** Astrocyte density in early human CPM cases (n=5) with significantly lower astrocyte density within lesion and higher density in perilesion. **c-d** Intermediate- (n=5) and late stage (n=8) CPM cases showing no significant differences between lesion, border or periplaque area (one-way- ANOVA).

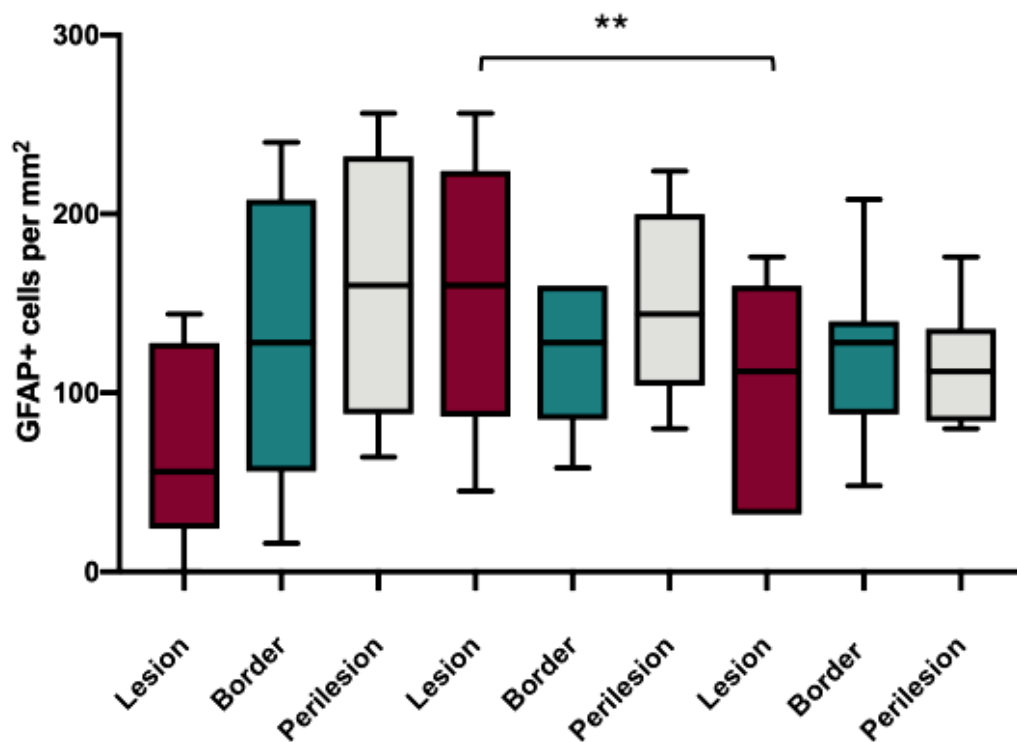


Fig. 8: Astrocyte density across early-, mid-stage and late-stage human CPM. Astrocyte density in lesion, border and perilesion across all lesion stages showing a highly significant difference between intermediate-stage (n=5, 4th-6th box) and late-stage (n=8, 7th-9th box) lesions (one-way ANOVA).

3.4.2 Astrocytes in CPM– morphological distinctions

We analysed the patient subgroups according to their astrocyte morphology, especially paying attention to so-called *bipolar astrocytes*. These are astrocytes with only one or two cell processes stretching to either side of the cell giving it a slender, elongated appearance (see Figure 6).

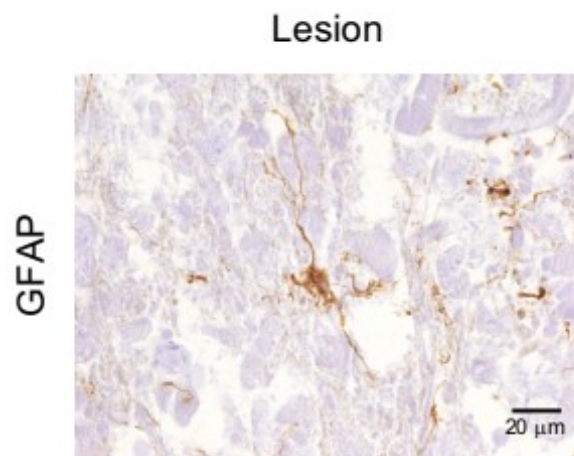


Fig. 9: Bipolar astrocyte in an early human CPM lesion. Patient no. 8. 400x magnification. Scale bar represents 20μm.

Bipolar astrocytes are thought to represent repopulating, regenerating astrocytes (Parratt & Prineas, 2010; Wrzos et al., 2014). We, therefore, hypothesized that there should be a higher fraction in recovering lesions, hence in early and intermediate CPM cases.

Indeed, we found a significant increase in bipolar astrocyte density within lesion (67.8 ± 19.5 bipolar GFAP+ cells/mm²) versus perilesion (11.4 ± 3.9) over the whole cohort (paired t-test, $p=0.0045$). After differentiating early, intermediate and late-stage CPM lesions, we found a significant difference between densities of bipolar

astrocytes in early versus intermediate CPM, or actively regenerating, cases compared to less bipolar astrocytes in late-staged human CPM cases, hence less actively regenerating (see Figure 10); (One-way ANOVA; $p=0.0332$). We could, further, demonstrate a significant and negative linear trend from high density of bipolar astrocytes in early lesions to a decreased density in late lesions (early stage: 122.8 ± 51.8 ; intermediate: 98.0 ± 30.5 and late-stage: 14.63 ± 4.9 ; One-way ANOVA; test for trend, slope: -56.04 ± 19.8 ; $p=0.0127$).

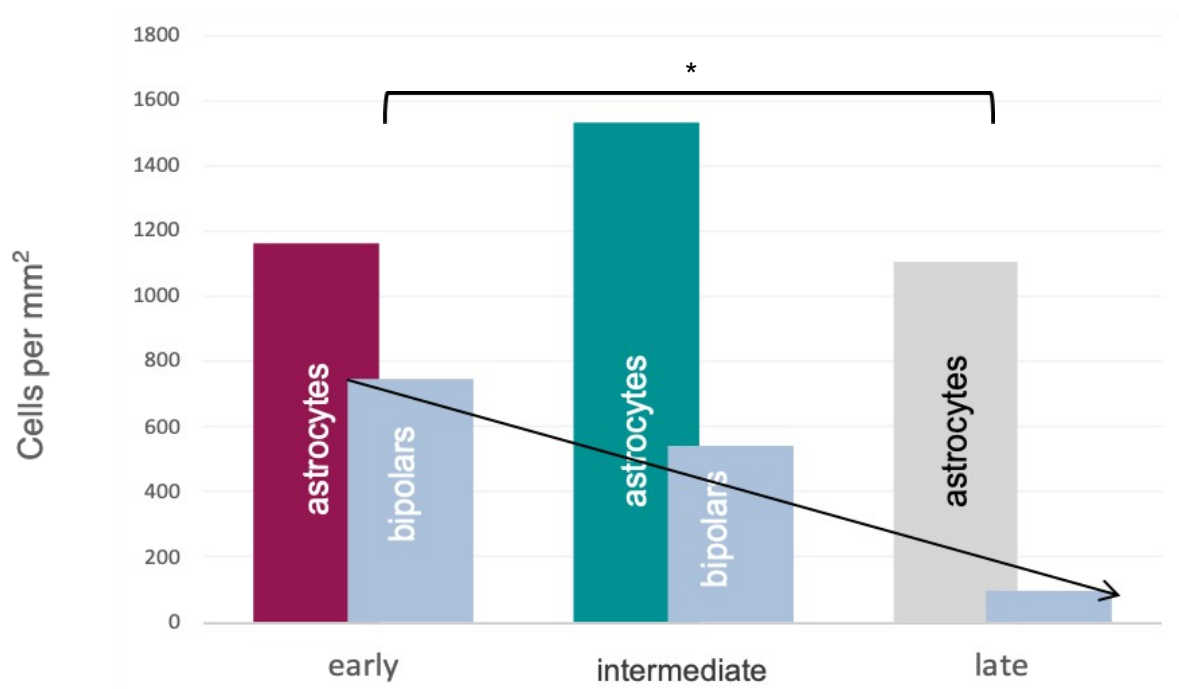


Fig. 10: Bipolar astrocytes in early, intermediate-stage and late-stage human CPM. Density of bipolar astrocytes within lesions of early ($n=5$), intermediate-stage ($n=5$) and late-stage ($n=8$) human CPM. The data presented demonstrate a significantly higher proportion of bipolar astrocytes within early CPM lesions compared to late stage, already remyelinated CPM lesions; $p=0.0127$ (one-way-ANOVA).

Across all stages of human CPM lesions, astrocytes demonstrated a more or less pronounced reactive morphology with abundant cytoplasm and numerous processes, which was more extensive closer to the lesion border than in the lesion center. This is known to be a feature of response to cellular- and osmotic stressors (Domingues et al., 2016). Figure 11 demonstrates the different morphological appearances of astrocytes from the initial development of a lesion until a later recovering stage. Early lesions show extensive astrocyte and AQP4 loss within lesions compared to perilesions and a high fraction of bipolar astrocytes. Early and intermediate lesions also demonstrate repopulation of bipolar astrocytes, which begin to re-express AQP4. In later staged lesions we found predominantly AQP4-positive astrocytes with denser and more elaborate morphology.

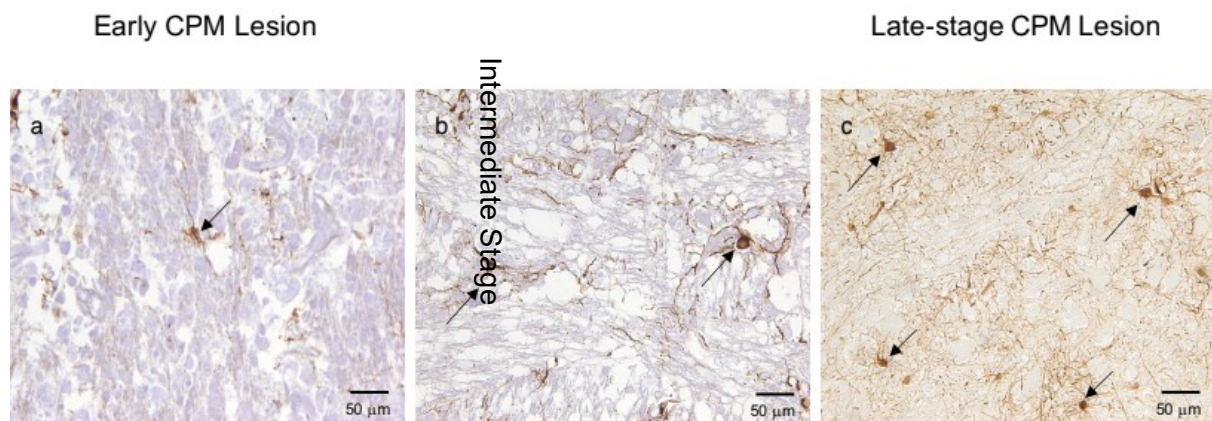


Fig. 11: Early, intermediate and late-stage CPM lesions stained for GFAP. 200x magnification; scale bar represents 50µm. **a** bipolar astrocyte within an early-stage CPM lesion (patient no 8). **b** dense, reactive and also bipolar astrocytes in an intermediate-stage CPM lesion (patient no 15). **c** multiple dense, round astrocytes with abundant processes in a late-stage CPM-lesion (patient no 3).

3.5 Oligodendrocyte densities within human CPM lesions

Considering the pattern of demyelination, gathered from the literature and our own experiments, we anticipated a reduced density of oligodendrocytes in lesion areas compared to perilesion. We, therefore, labelled mature oligodendrocytes using p25 IHC together with LFB staining. We were, thus, able to determine the mean oligodendrocyte density within the demyelinated or remyelinated lesion. We then compared the overall density of oligodendrocytes within CPM lesions with their densities at the lesion border and the perilesion. We found a highly significant difference between the densities of oligodendrocytes in lesion versus perilesion 117.1 ± 28.9 and 293.9 ± 26.31 p25 positive cells/mm², respectively (paired t-test; $p < 0.0001$). In accordance with our hypothesis on lesion formation in human CPM, we could show that the density of mature oligodendrocytes was significantly reduced within lesions compared to perilesional areas over the entire course of lesion evolution (Figure 12).

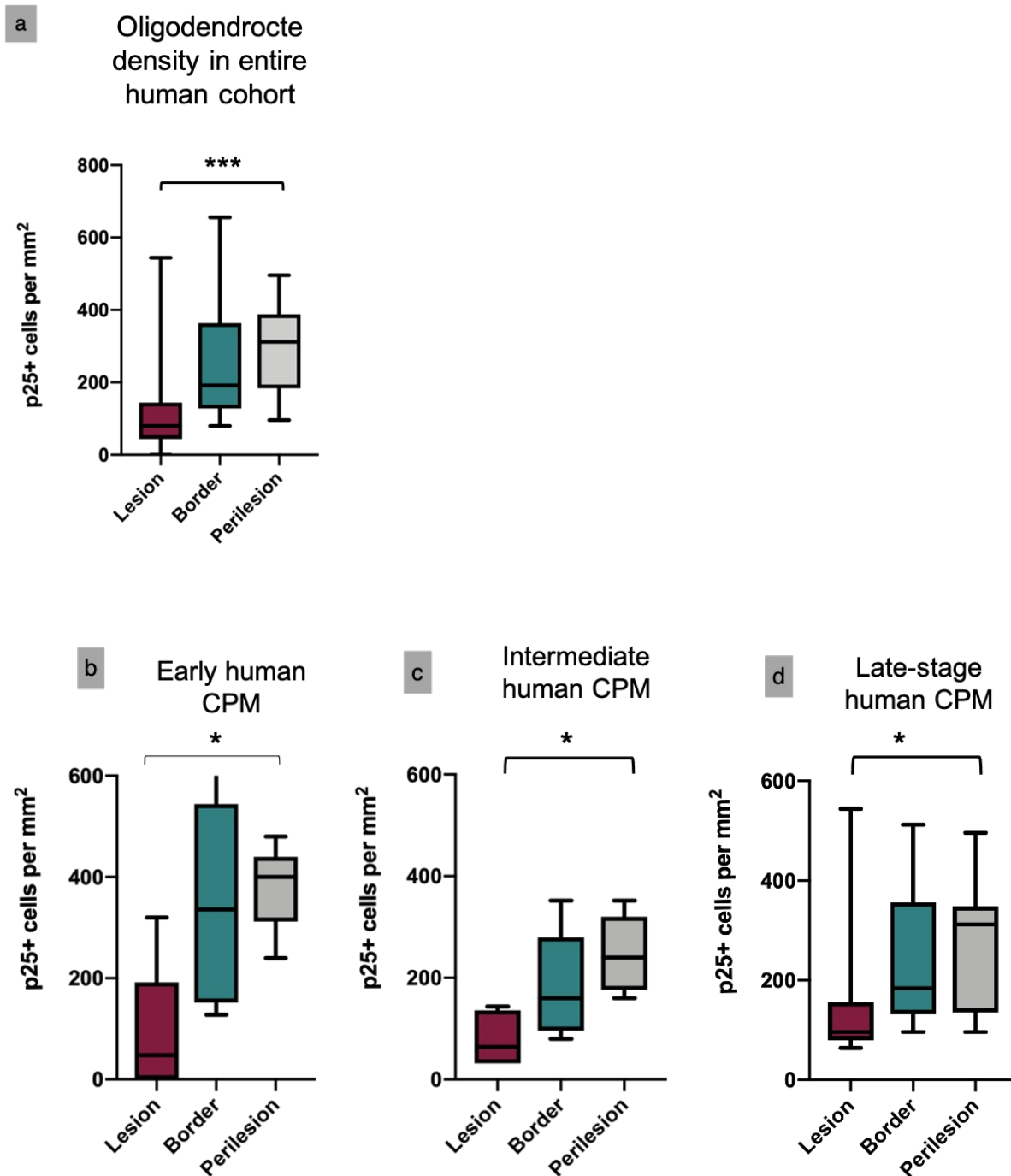


Fig. 12: Oligodendrocyte density in early-, intermediate- and late-stage human CPM.

a Oligodendrocyte density in lesion, lesion border and perilesion showing a highly significant difference between lesion and perilesion over the entire cohort. **b** Significantly reduced oligodendrocyte density in early human CPM lesions compared to higher densities in the perilesion. **c** intermediate-stage CPM cases demonstrating a significantly reduced density between lesion and periplaque area **d** late-stage CPM cases showing a significantly reduced density between between lesion and periplaque area. Stained against p25+. one-way ANOVA.

We analysed our data according to the different stages of lesion evolution and found a statistically significant difference between the densities of p25 positive oligodendrocytes in early lesions compared to early perilesional areas with cell densities of 86.4 ± 59.8 and 380.8 ± 39.9 respectively (one-way ANOVA $p=0.0107$, Tukey post-hoc). We found a significant linear trend from lesion over border to perilesional densities of oligodendrocytes (one-way ANOVA; slope: 147.2 ± 40.88 ; $p=0.0070$). The densities of intermediate- and late-stage cases also revealed a statistically significant difference between lesion and perilesion densities as well as a significant linear trend from lesion over border to perilesional densities of oligodendrocytes (intermediate stage lesion versus perilesion: 80.0 ± 23.7 and 246.4 ± 34.2 ; one-way ANOVA $p=0.0290$; slope: 83.20 ± 23.01 ; $p=0.0068$ and late-stage lesion versus perilesion: 154.7 ± 49.82 and 272.0 ± 42.42 ; one-way ANOVA $p=0.0229$; slope: 58.67 ± 14.72 ; $p=0.0011$). Noteworthy, over lesion development the steepness of this trend flattens, possibly as with regeneration lesion and perilesional oligodendrocyte densities converge. Figure 13 below depicts the density and morphology of oligodendrocytes within lesions, compared to border and perilesion. There was no significant difference in oligodendrocyte densities between early- intermediate- and late-stage lesions, however, densities gradually increased from early towards later-stage lesions but did not reach perilesional levels.

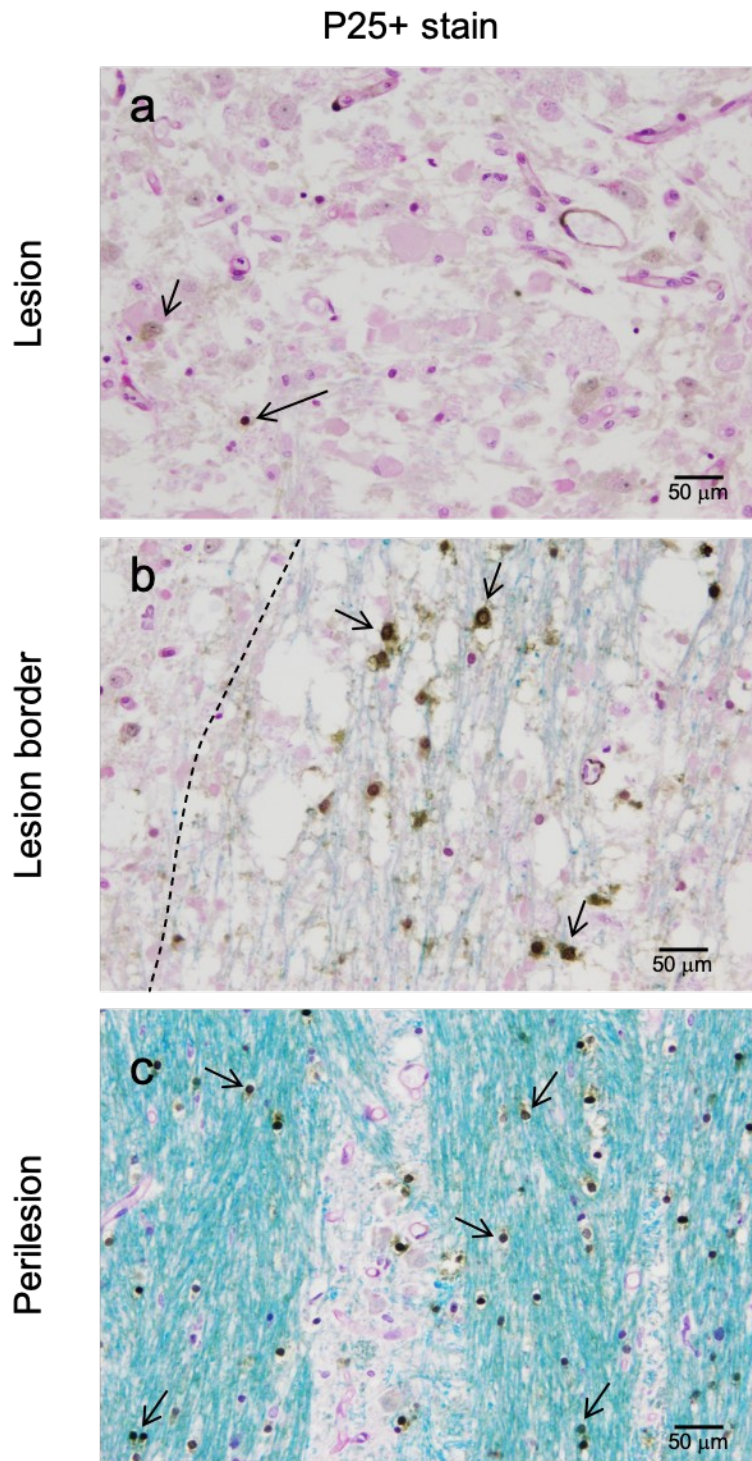


Fig. 13: Oligodendrocyte density in early CPM lesions.

Myelin (LFB; blue); mature oligodendrocytes (p25 IHC; brown). **a** Striking loss of oligodendrocytes within early lesions. **b** Oligodendrocyte density at the lesion border. The dashed line separates lesion on the left and lesion border on the right. **c** Oligodendrocyte density in the perilesion showing regular densities. 200x magnification; scale bar represents 50 μm.

Morphologically, oligodendrocytes within early and intermediate lesions showed hallmarks of injury like chromatin hypercondensation or nuclear fragmentation. In late-stage cases, oligodendrocytes often still showed abnormal morphology with swollen cell bodies.

The interdependence of astrocytes and oligodendrocytes is well known and backed up by current research (Domingues et al., 2016). As demonstrated in Figure 14, we found a trend for a positive correlation between the densities of astrocytes and oligodendrocytes in early lesions ($r: 0.821$; $p=0.088$; Pearson correlation).

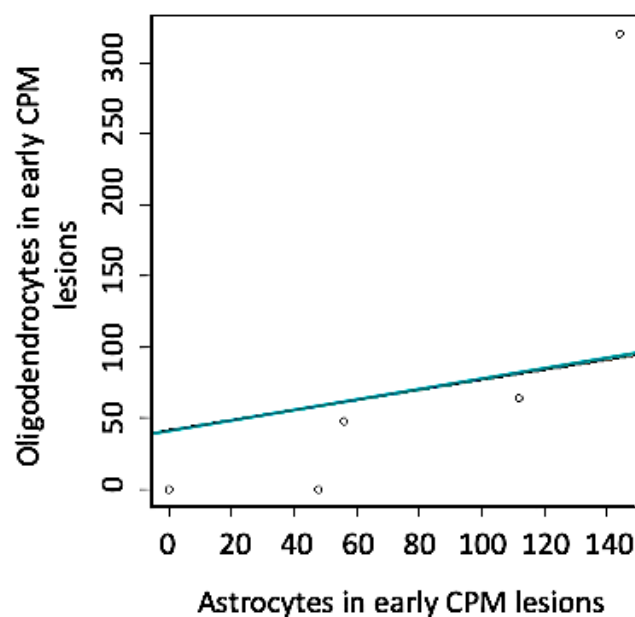


Fig. 14: Correlation of astrocyte and oligodendrocyte density in early lesions. Trend for a positive correlation between densities of astrocytes and oligodendrocytes in early lesions; $r: 0.821$; $p=0.088$; Pearson correlation.

Astrocyte and oligodendrocyte densities showed different dynamics according to lesion stage, in which oligodendrocytes showed a marked increase in late stage, while astrocytes had the maximum density in intermediate stage (Figure 15).

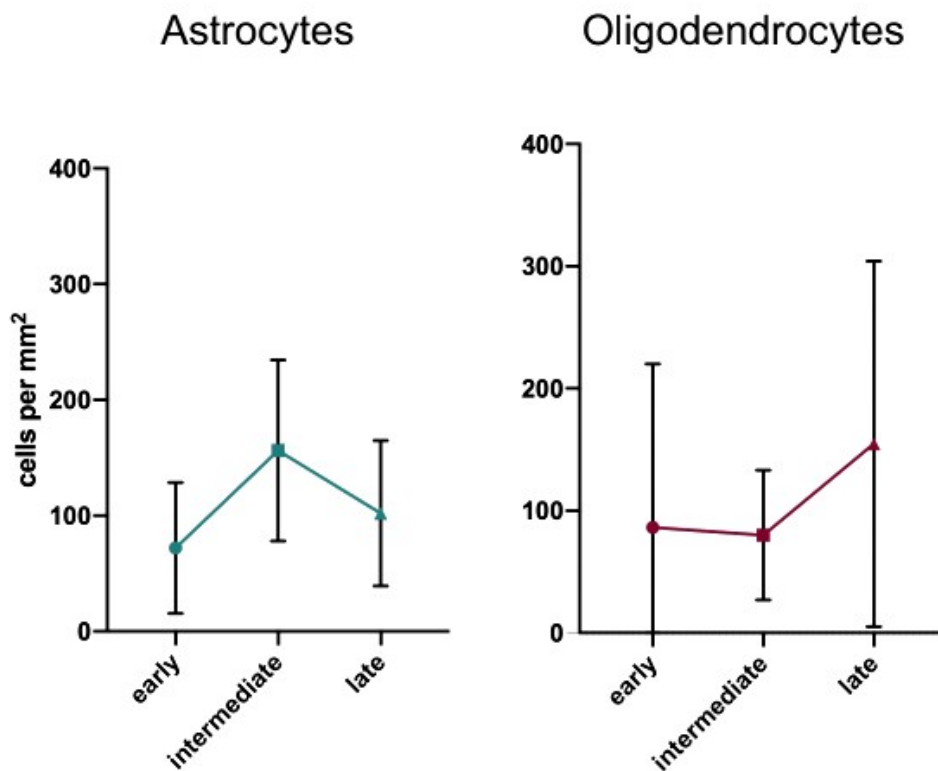


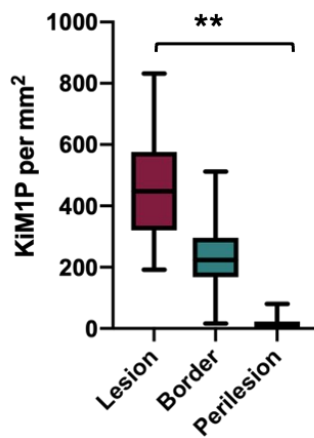
Fig. 15: Astrocyte and Oligodendrocyte density in early, intermediate- and late-stage lesions. Astrocyte and oligodendrocyte densities shown as mean density of cells per mm² demonstrating different dynamics according to lesion stage.

3.6 Macrophages and activated microglia

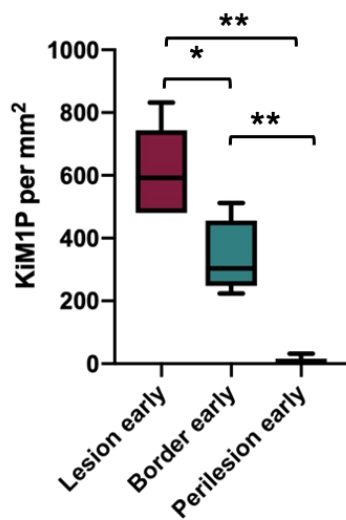
3.6.1 KiM1P – a marker for infiltrating macrophages and activated microglia

We quantified the density of macrophages/activated microglia via KiM1P-IHC in the same areas on consecutive sections and saw significantly higher densities of KiM1P+ cells/mm² in lesions compared to lesion border and perilesion (457.4±44.7; 239.1±27.4 and 12.1 ±5.2; One-way ANOVA p<0.0001, Tukey post-hoc). As with the other markers we could demonstrate a significant linear trend from lesion over border and perilesional densities of macrophages/activated microglia across the whole cohort (one-way ANOVA; slope: -222.7±22.7; p<0.0001). A similar trend was observed within the subgroups: early-stage lesion versus perilesion: 608.0±65.4 cells/mm² vs. 6.4±6.40 cells/mm²; one-way ANOVA p=0.0021; slope: -300.8±28.8; p=0.0001; intermediate-stage lesion versus perilesion: 352.0±68.8 cells/mm² and 19.2±15.5 cells/mm²; one-way ANOVA p=0.00095; slope: -166.4±33.4; p=0.0068 and late-stage lesion versus perilesion: 425.1±66.6 cells/mm² versus 9.625±5.0 cells/mm²; one-way ANOVA p=0.0017; slope: -207.0±29.3; p<0.0001)

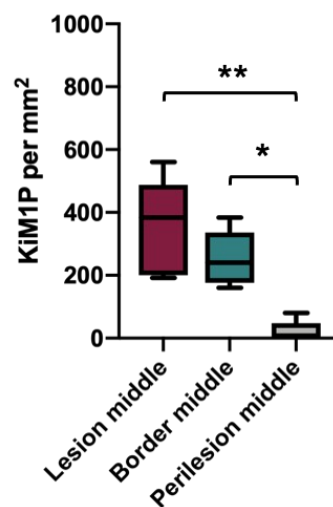
a KiM1P+ macrophages
in whole cohort of human
CPM



b Early human CPM



c Intermediate-stage
human CPM



d Late-stage human
CPM

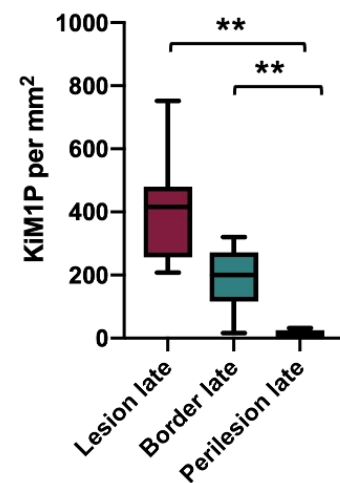


Fig. 16: Density of KiM1P positive macrophages/activated microglia in early-, intermediate- and late-stage human CPM.

a KiM1P-positive macrophages/activated microglia density in lesion, border and perilesion showing a highly significant difference between lesion and perilesion over the whole cohort. **b** significantly increased density of KiM1P positive macrophages in early human CPM lesions compared to a less pronounced increase at the border and few cells in the perilesion. **c** intermediate-stage CPM cases also demonstrating a significant difference between KiM1P positive macrophages with high densities in the lesion, compared to a less pronounced increase at the border or periplaque. **d** Late-stage CPM cases still showing a significant difference of KiM1P positive macrophages within lesions compared to periplaque area. One-way ANOVA.

Moreover, when analyzing the tissue samples stained for KiM1P, we found not only pronounced infiltration into lesions but also evidence of activated foamy macrophages with phagocytosed myelin debris in early and intermediate-stage lesions (Figure 18). In late-stage lesions, the macrophages were roundish, somewhat smaller, and did not demonstrate ongoing phagocytosis.

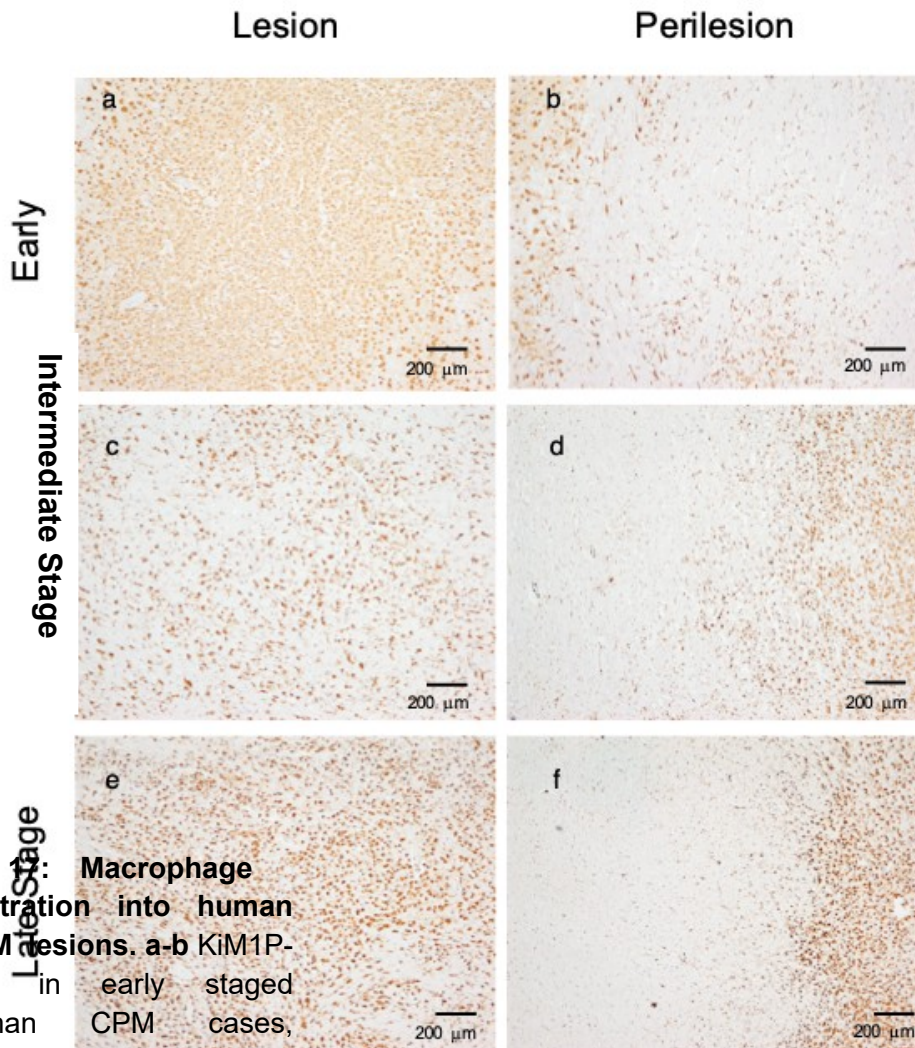


Fig. 1: Macrophage infiltration into human CPM lesions. **a-b** KiM1P-IHC in early staged human CPM cases, showing activated foamy macrophages/activated microglia in the lesion area indicating phagocytosis (**a**), but not in the perilesion area (**b**); patient no 8. **c-d** IHC against KiM1P in intermediate-stage lesions, marking activated foamy macrophages/activated microglial cells in the lesion area (**c**), but almost none in the perilesion area (**d**); patient no 4. **e-f** IHC against Kim1P, marking dense round macrophages/activated microglial cells in the lesion area (**e**), but not in the perilesion area (**f**); patient no 2. 40x magnification, scale bar represents 200 μm .

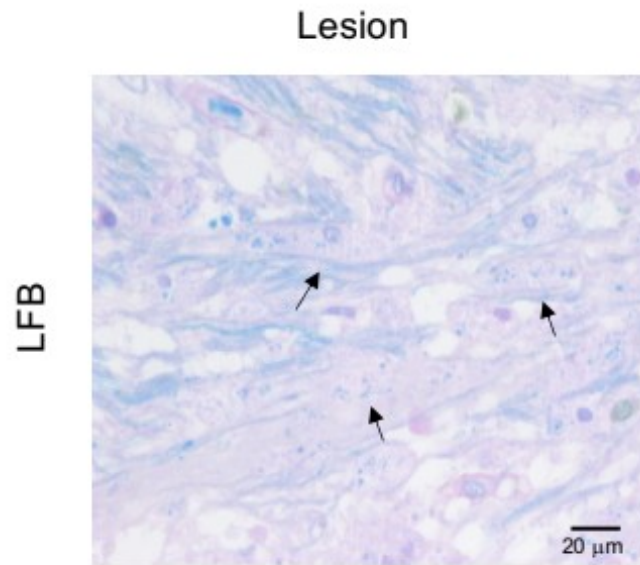


Fig. 18: Early-stage CPM lesion with myelin-phagocytosing macrophages.

Patient no 6. 400x magnification; scale bar represents 20μm.

3.6.2 Proliferating Iba1+ cells are observed in all lesion stages

The marker *Ionized calcium binding adaptor molecule 1* (Iba1) is a microglial and macrophage-specific protein. Iba1 stains all microglia, “resting”, activated and also infiltrating monocytes and macrophages. We quantified the density of proliferating microglia using double immunohistochemistry against Iba1 and Ki67 and observed a

significant increase in the number of Ki67+ proliferating macrophages/microglia in lesion areas compared to perilesion. In lesions, the mean density of proliferating Iba1-positive cells was significantly increased (13.2 ± 2.6 Iba1+ cells/mm²) compared to perilesional areas which had a mean density of 5.3 ± 1.2 Iba1+ cells/mm² (paired t-test; $p=0.0007$). Figure 19a demonstrates the density of proliferating macrophages/microglia in lesion versus perilesion across the entire cohort of human CPM cases demonstrating a highly significant difference. Figures 19b-d depict the density of proliferating macrophages/microglia in lesion versus perilesion and broken down into the early, intermediate- and late-stage human CPM cases where no statistical significance was found in early and intermediate stage-lesions. In late-stage lesions a significantly higher density of proliferating macrophages/microglia in lesions compared to perilesions was seen (Fig. 19).

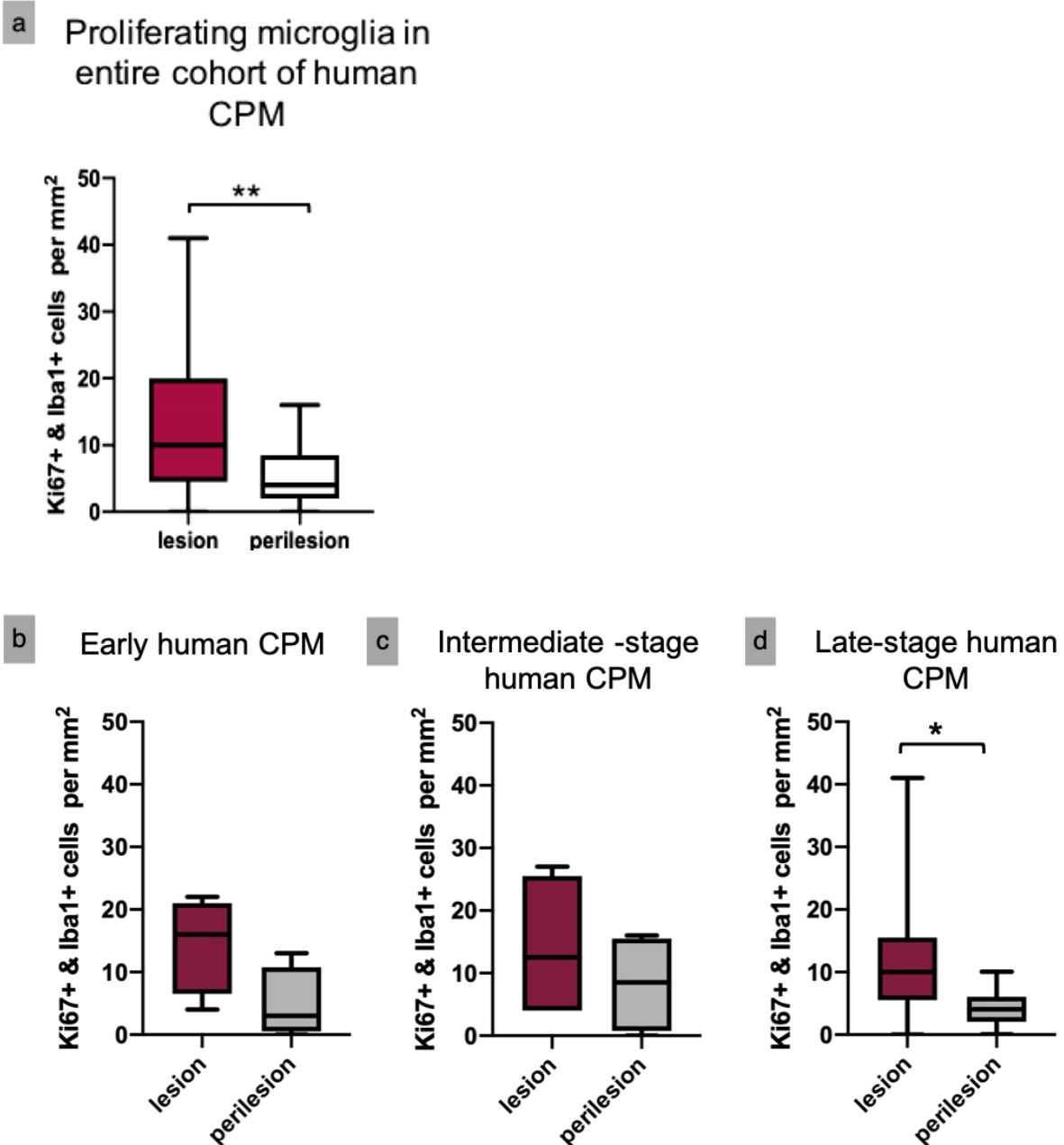


Fig. 19: Density of proliferating Iba1/Ki67 double positive macrophages/microglia in early-, intermediate- and late-stage human CPM. a Iba1/Ki67-double positive macrophages/microglia are significantly increased in CPM lesions; paired t-Test. **b** Higher numbers of proliferating macrophages/microglia in early lesions compared to the perilesion, though not reaching significance. **c** Intermediate-stage CPM cases also demonstrating higher densities of proliferating macrophages/microglia in the lesion, but similarly not reaching significance. **d** Late-stage CPM cases showing a significantly higher density of proliferating macrophages/microglia within lesions versus perilesion; paired t-Test.

4 Discussion

Damage to the panglial syncytium is a common mechanism of myelin loss in demyelinating diseases of the CNS (Rash, 2010; Stadelmann et al., 2019). The relation between astrocyte pathology and demyelination has been established in osmotic demyelination and other demyelinating disorders (Bouchat et al., 2018, 2018; Gankam Kengne et al., 2011; Kleinschmidt-Demasters et al., 2006; Kleinschmidt-DeMasters & Norenberg, 1981; Nicaise et al., 2019; Ponath et al., 2018; Popescu et al., 2013). However, the mechanisms of lesion repair in the context of astrocyte dysfunction and loss remain mostly elusive. To infer a timeline in terms of astrocyte- and oligodendrocyte destruction and recovery in human CPM, we analysed tissue from a cohort of patients who died with CPM and related our data to the literature and to studies in experimental animals.

4.1 Lesion Staging

Experimental results in animal models of ODS suggest that loss of astrocytes, as well as oligodendrocytopathy, is observed within 24 hours after rapid correction of chronic hyponatraemia. While demyelination is detected within 48 hours and neurons and axons are spared (Bouchat et al., 2018; Illowsky & Laureno, 1987; Kleinschmidt-DeMasters & Norenberg, 1981; Laureno, 1983). Astrocytes play a fundamental role in osmolar regulation in the CNS and, therefore molecules directly involved in this process, for instance the water channel AQP4, are thought to mediate pathogenesis in CPM (Mader & Brimberg, 2019; Popescu et al., 2013). AQP4 transporters are water channels found on astrocytic endfeet especially involved in brain water and

electrolyte homeostasis as well as in clearance of cell debris and maintaining the blood-brain barrier (BBB). Astrocytes and AQP4 channels have been shown to play a central role in other demyelinating pathologies, e.g. neuromyelitis optica, where autoantibodies target AQP4, or in MS where reactive astrocytes play a role in the inflammatory and neurotoxic processes (Mader & Brimberg, 2019; Parratt & Prineas, 2010; Popescu et al., 2013).

Microscopic analysis of our patient cohort revealed the numerous abnormalities known to be associated with the ODS. Besides loss of myelin, we found changes in astrocyte density, morphology and AQP4 expression as well as reduced or damaged oligodendrocytes. Based on the current literature and our previously published study in an animal model of CPM, we divided the cohort into three stages and in particular analysed astrocytes, myelin, oligodendrocytes and macrophages. For lesion staging, we analysed our cases according to the criteria already discussed earlier and grouped similar samples. Of the 18 CPM cases with clear pontine lesions, five met the criteria for early- (n=5), five for intermediate- (n=5), and eight for late-stage lesions (n=8).

Early-stage lesions demonstrated a confluent and complete loss of myelin by LFB staining and myelin protein immunohistochemistry (IHC). The density of astrocytes was significantly reduced in early-stage lesions compared to the perilesion, with some clasmatodendrosis as a sign of astrocyte damage. Astrogliosis was predominantly observed at the lesion edge. The few astrocytes present in the lesion center were mostly bipolar and AQP4 negative, indicating that these had recently repopulated (Popescu et al., 2013). This is in line with observations by Bouchat et al. in an animal model of ODS (Bouchat et al., 2018). Furthermore, a dense infiltration of

foamy Kim1P-positive macrophages/activated microglia was observed of which some phagocytosed myelin debris, as shown by the presence of LFB in macrophages. Thus suggesting that lesions with lowest density of astrocytes and clear-cut borders represent early-stage CPM. The complete myelin loss in our cohort of human post-mortem cases indicates that lesions are later in lesion development compared to early-stage lesions in animal models, where myelin is still preserved at least until day 3 after lesion induction (Lohrberg 2020). However, these extremely early stages were not represented in our cohort. In early lesions, in line with previously published work and also data from our experimental ODS lesions, oligodendrocytes, as cells responsible for CNS myelin maintenance, were significantly reduced compared to the perilesion across all lesion-stages (Lohrberg et al., 2020). Oligodendrocytes, further, showed features of injury such as chromatin hypercondensation and fragmentation. In a rat model, these changes were accompanied by swollen organelles and degradation of the nucleus with interchromatin granules (Bouchat et al., 2018).

Intermediate-stage lesions showed a slightly increased density of astrocytes compared to the perilesion that were mainly AQP4 positive. This expression of AQP4, however, was more pronounced closer to the lesion border, and three cases were AQP4 negative in the very center of the lesion. Astrocyte morphology was frequently ramified, less often bipolar, suggesting advanced astrocyte repopulation of the lesion area. From basic research on astrocyte development, it is known that astrocytes first develop long, less ramified processes, which then grow out centrifugally into finer processes (Heller & Rusakov, 2015). The morphology of astrocytes was also analysed by Wrzos et al., who described proliferating astrocytes showing a bipolar morphology as an indication of astrocyte repopulation in NMO

(Wrzos et al., 2014; Parratt & Prineas, 2010). Newly formed astrocytes are bipolar early on, ramify in the course of development and (re-) express AQP4 with time. We concluded that ramified AQP4+ astrocytes are already further along the line of lesion repair. Intermediate-stage lesions still show extensive demyelination and slightly reduced densities of oligodendrocytes within lesions compared to early-stage lesions. One interpretation could be ongoing cell death or hindered maturation of oligodendrocytes due to lack of astrocyte-derived survival, proliferation and differentiation factors, such as platelet-derived growth factor (PDGF) (Gard et al., 1995; Lohrberg et al., 2020; Moore et al., 2011; Pringle et al., 1989). It also indicates that OPC proliferation and differentiation into myelinating oligodendrocytes do not yet occur at this lesion stage (Baaklini et al., 2019; Hammond et al., 2014; Zhang et al., 2009). Recently, our group could show that OPCs fail to differentiate into actively remyelinating oligodendrocytes in the absence of astrocytes in experimental ODS. Furthermore, our work demonstrated that OPCs do not regain their full remyelination capacity even after recovery from the osmotic stress and, at least in the rat model, need support from OPCs that migrated from neuronal stem cell niches like the subventricular zone (Lohrberg et al., 2020). Also, other groups, for example Talbott et al., demonstrated the necessity of astrocytes for the remyelination capacity of OPCs in a rat model (Talbott et al., 2005). It can be deduced that the lack of nutritive support due to the immature astrocytes is one explanation for the incomplete differentiation of pre-myelinating oligodendrocytes into mature and myelinating oligodendrocytes. Even though more data on the effect of astrocyte-derived survival factors on OPCs/ oligodendrocytes are emerging, the fate of OPCs in human CPM lesions requires further studies.

The late-stage human cases analyzed still showed macrophages/activated microglia within the lesion and LFB was absent or showed evidence of remyelination. Astrocytes showed densities comparable to the perilesion with regular expression of AQP4 and a star-shaped, reactive, but not bipolar, morphology. Even though oligodendrocyte densities were highest of all lesion stages, densities remained reduced compared to the perilesion and the normal-appearing white matter.

4.2 Astrocytes in the pathogenesis of CPM

One possible interpretation of our findings is that lesion formation in CPM follows an “inside out” fashion, spreading from the cell body of astrocytes (and AQP4-rich astroglial endfeet) over to oligodendrocytes and inducing damage and dysfunction, possibly by the release of toxic cytokines or, indirectly, by the lack of growth factors. After oligodendrocyte death, this process cumulates in the breakdown and then phagocytosis of myelin. Emerging research supports our hypothesis on the vital role of astrocytes in initiating the cascade of events resulting in the development of ODS lesions (Nicaise et al., 2019), which is consistent with studies on animal models (Bouchat et al., 2018; Gankam Kengne et al., 2011; GankamKengne et al., 2017; Lohrberg et al., 2020; Traka et al., 2016; Weil et al., 2016; Wrzos et al., 2014).

Besides evidence on the production of pro-inflammatory cytokines in reaction to osmotic stress, the central role of astrocytes in the regulation of homeostasis and CNS development is well established (Mader & Brimberg, 2019; Zuchero & Barres, 2015).

Moreover, in experimental models of MS, in particular experimental autoimmune encephalomyelitis (EAE), it was shown that molecules released by astrocytes may

contribute to oligodendrocyte demise. Among others, hyaluronan and astrocyte-derived endothelin-1 (ET-1) hinder OPC differentiation and remyelination as well as microglia attraction and activation (Back et al., 2005; Brambilla et al., 2009; Correale & Farez, 2015; Domingues et al., 2016; Hammond et al., 2014; Huang et al., 2001). The following invasion of macrophages and recruitment of microglia further supports the generation of an inflammatory environment in the lesion. Also, the production of proinflammatory cytokines by macrophages/activated microglia might contribute to the interplay between astrocytopathy and oligodendrocyte loss. As astrocytes fulfill a glutamate scavenging function, their loss results in accumulation of this cytotoxic substance which in turn leads to oligodendrocyte death (Bannerman et al., 2007). Finally, disruption of the BBB results in circulation of even more immune factors which exaggerates the immune response (Baker et al., 2000).

Due to the crucial role of astrocytes in regulating homeostasis at the gliovascular interface, it is of great importance to analyse the interdependence of astrocytes, their water channel *AQP4* and the brain's water/ion exchange in the pathogenesis of demyelinating diseases (Maria Teresa Gentile, 2018).

As described in the chapter on lesion staging, we could demonstrate a change in *AQP4* expression over the course of lesion development. In line with our data, Popescu et al. also found that *AQP1* and *AQP4* immunoreactivity was lost in four of their six actively demyelinating lesions on human CPM. Curiously, while these four patients were male, the two females had elevated *AQP1* and *AQP4* immunoreactivity and marked astrogliosis. Popescu et al. proposed the idea of *AQP* loss as a protective measure to prevent astrocyte apoptosis. On the other hand, upregulation of aquaporins might aid in water removal in vasogenic edema. Following this chain of

thought, they brought up the relevance of male or female sex hormones for the expression of ion and water channels. As it was already described in animal models that sex hormones can exert opposite effects on ion transporters and also that oestrogen induces expression of AQP, they hypothesised that loss of AQP1 and AQP4 might be restricted to male CPM patients, or associated with confounding factors of CPM more common in men (Akaishi & Sakuma, 1990; Fraser et al., 1989; Popescu et al., 2013; Zou et al., 2013). Conversely, female sex hormones might serve as protective factor against AQP loss, or females may have different underlying conditions that protect from aquaporin loss. However, they acknowledged that their sample of six human CPM cases was relatively small and therefore precludes definite statements about the relevance of sex hormones in this regard. In our cohort we could not demonstrate a correlation between sex and AQP expression.

Lesion repair is reflected in different astrocyte morphologies along the stages of lesion evolution. So far, little is known on astrocyte regeneration in human CPM. However, in previous research on NMO, where astrocytes are the primary target of the pathogenic events, a consistent timeline of astrocyte repopulation has been demonstrated. Bipolar astrocytes in early lesions proliferate, differentiate, ramify and re-express AQP4 in intermediate- and late-stage lesions. Bipolar astrocytes were mostly seen in early and intermediate-stage lesions which is in line with studies showing repopulation of AQP4-positive astrocytes during lesion recovery. It is hypothesized that during recovery, AQP1 and AQP4 channels support the re-establishment of homeostasis and have, thus, a favourable influence on lesion repair (Gankam Kengne et al., 2011; Lohrberg et al., 2020; Popescu et al., 2013).

Parrat and Prineas demonstrated bipolar astrocytes in early human NMO lesions, but did not assess oligodendrocyte remyelination (Parratt & Prineas, 2010). They showed that during the evolution of NMO lesions, following reduction of astrocytes and absence of AQP4 immunoreactivity, bipolar AQP4-negative astrocytes re-appear and differentiate into AQP4-positive differentiated astrocytes (Parratt & Prineas, 2010). These findings were later supported by studies in MS and NMO lesions where repopulation of bipolar astrocytes shortly after lesion initiation was seen (Brück et al., 2012; Wrzos et al., 2014). The research by Prineas and Lee on astrocyte pathology in early MS lesions further underpinned these findings. They observed that “the proportion of newly generated stellate GFAP-positive astrocytes that are also AQP4-positive increases with time” in early multiple sclerosis lesions (Prineas & Lee, 2019). It is conceivable that astrocytes that are still proliferating demonstrate a rounder morphology and only start generating bipolar extensions once active proliferation has stopped.

The crucial role of astrocytes in a wide variety of homeostatic processes, promoting neuronal survival and protection by nutritive functions as part of the BBB, is well known (Mader & Brimberg, 2019; (Ponath et al., 2018).

Our study demonstrated an increase in astrocyte density from the lesion center with few astrocytes, the border with more and the periplaque area with the highest mean density of astrocytes per mm². Interestingly, we also found an increase in astrocyte density from early to intermediate-stage lesions, followed, however, by a statistically significant reduction of astrocytes from intermediate-stage to late-stage lesions. This might be explained by active proliferation, endorsed by the bipolar and ramified morphology of astrocytes in the early and intermediate-stage lesions and extensive

astrogliosis in earlier CPM lesions which recedes in later stages (Zuchero & Barres, 2015). When comparing all stages, astrocytes appear reactive with abundant cytoplasm and numerous projections. In early lesions this reactivity is more pronounced at the edge of the lesion as compared to the centre. In intermediate stages, astrogliosis is present also closer to the lesion center, astrocytes generally appear increasingly ramified and bipolar, whereas in later staged lesions which are partly remyelinated, astrocyte densities are comparable to perilesional areas, and the cells appear denser with a round morphology and fewer ramifications. As astrogliosis subsides and calms from the edges of the lesion to the centre, the number of astrocytes may also recede.

In our work, astrocytes generally demonstrated higher densities towards the perilesion and so did oligodendrocytes which showed a maximal density closer to the lesion border. Both cell lineages decreased gradually towards the lesion centre supporting the hypothesis of repopulation from the periplaque area/lesion border. Further, expression of AQP4 also seemed to spread from the lesion border towards the center. It was shown that not only the loss of oligodendrocytes follows astrocyte loss, but also the repopulation of oligodendrocytes seems to follow the repopulation of astrocytes (Figure 15). However, it has to be said that even if oligodendrocytes repopulate throughout CPM, their density remains reduced compared to the perilesion in late-stage CPM.

4.3 Oligodendrocyte pathology in CPM

In this study, we demonstrated that oligodendrocytes were significantly reduced within lesions compared to the perilesion area over the entire cohort.

Morphologically, the remaining oligodendrocytes were shrunken and partly presented fragmented nuclei, in particular in early lesions which aligns with previously published research (Bouchat et al., 2018, Newell & Kleinschmidt-DeMasters, 1996; Nicaise et al., 2019). When analysing the different lesion stages separately, we found a significant reduction in oligodendrocyte density in lesions compared to perilesions. Further, we found a higher, although not significant, oligodendrocyte density in late-stage- compared to early-stage lesions. Although some recovery can be assumed, oligodendrocyte density was far from reaching perilesional/healthy levels. However, this increase may indicate repopulation with oligodendrocytes through proliferation and differentiation of local oligodendrocyte progenitor cells (OPCs). Another hypothesis is that oligodendrocytes derived from neural stem cells contribute to oligodendrocyte repopulation as observed in the rat model in human pontine CPM lesions (Lohrberg et al., 2020).

As already described earlier oligodendrocyte loss and astrocytopathy are spatially and timely correlated – initiated and possibly perpetuated by the secretion of cytokines by reactive astrocytes and/or microglia as well as loss of communication pathways between the cell lineages. Proinflammatory cytokines are more likely released by the activated microglia/macrophages present in enormous amounts in early and intermediate lesions than by the reduced number of astrocytes. It was already established in research on MS that inflammatory cytokines like TNF- α and IL-1 β damage oligodendrocytes and hinder remyelination (Cammer, 2000). On the other hand, studies in rats demonstrate reduced demyelination and clinical symptoms upon interventions that inhibit microglia activation or inflammatory cytokines directly. For example, Takefuji et al. and also Gankam-Kengne et al. demonstrated that the

blockage of proinflammatory cytokines like TNF- α and IFN- γ as well as iNOS, IL1 α and protein nitrosylation by lovastatin or minocycline had a protective effect in ODS animal models in that demyelination, neurological deficits and also mortality was significantly improved compared to controls (Gankam-Kengne et al., 2010; Takefuji et al., 2007). Though, experimental evidence supports a detrimental influence of activated microglia and proinflammatory cytokines in progression of demyelination, also beneficial effects of microglia activation have been reported and will be discussed at a later stage.

Some studies focus on the role of oligodendrocyte apoptosis in osmotic demyelination. Oligodendrocytes are particularly vulnerable to shifts in osmolality and often react with apoptosis to an excessive loss of osmolytes and water (Bouchat et al., 2018; Choi et al., 2014; Nicaise et al., 2019). Ashrafian et al. and De Luca et al., for example, demonstrated the activation of apoptotic pathways in response to osmotic stress (Ashrafian & Davey, 2001; DeLuca et al., 2002). The team of De Luca et al. was able to show a rise in apoptosis-related markers like Bax, Bim, Bak and death receptor 3 in glia cells after an osmotic insult (DeLuca et al., 2002). In line with these findings, Martin et al. raised the question whether the “unintentional” recruitment of a specific potassium channel in oligodendrocytes experiencing osmotic stress is involved in triggering the apoptotic cascade (R. J. Martin, 2004). In our study, we did not specifically stain for apoptotic markers. However, we found condensed and fragmented oligodendrocyte nuclei within lesions which might be seen as an indicator for apoptosis and would align with the above-mentioned work.

Other studies consider oligodendrocyte loss and demyelination to be secondary to defective glial proteostasis/protein folding in response to osmotic stress (Gankam-

Kengne et al., 2017) and most experimental models of CPM suggest that oligodendrocytopathy follows astrocyte loss.

Also, it has been suggested that both cell lineages, astrocytes and oligodendrocytes, react simultaneously to osmotic stress, but undergo different forms of cell death, e.g. rapid necrosis and a form of delayed apoptosis. However, this hypothesis cannot easily be tested in human tissue. Even if it is feasible to create a rough timely sequence of lesion formation and, therefore, gain an understanding of pathological stages in human CPM our preferred interpretation that oligodendrocyte loss is secondary to astrocytopathy is biased. It is also conceivable that both cell types are simultaneously and severely damaged at the time point of the osmotic insult.

4.4 Mechanisms of regeneration in human CPM lesions

The link between astrocyte pathology and lesion formation in demyelinating diseases of the central nervous system has been addressed by several groups. As discussed in more depth in the previous chapters, the crosstalk between astrocytes and oligodendrocytes was of intense research interest over the last decades and highlighted its necessity for migration, differentiation and remyelinating capacity of oligodendrocytes within demyelinating lesions.

Interestingly, the cells involved seem to play different roles at different stages of lesion evolution. From initiating/perpetuating demyelination towards resolution and regeneration at later stages. Astrocytes in particular seem to fulfill a dual role, beneficial as well as detrimental, in the process of remyelination at different stages of demyelinating pathologies (reviewed recently by (Rawji et al., 2020)).

On the one hand, it was shown that the secretion of inhibitory molecules and proinflammatory factors by astrocytes hinders oligodendrocyte maturation and thus remyelination. Multiple studies over the last years proved a detrimental role of astrocytes in remyelination. For example, Hammond et al. demonstrated, in an MS model in rats and via knockout of endothelin-1, an increased expression of *ET-1* by reactive astrocytes and *Jagged1* and in turn activation of *Notch* signaling in oligodendrocytes. They, further, showed that the rate of oligodendrocyte differentiation and remyelination was significantly reduced (Hammond et al., 2014). Another study in the EAE mouse model of MS by Back et al. highlighted the inhibitory function of hyaluronan that is secreted by astrocytes in demyelinating lesions after injection of lysolecithin (Back et al., 2005). A1-Astrocytes, a kind of neurotoxic astrocyte-subtype, even secrete molecules that are directly toxic to oligodendrocytes. This was demonstrated in a mouse model of neuroinflammation and ischemia by Liddel et al. (Liddel et al., 2017).

On the other hand, already in 1991, Franklin et al. demonstrated that the transplantation of type-1 astrocytes supports oligodendrocytes and myelination in the ethidium bromide model of demyelination in rats. After induction of demyelination, they transplanted purified type-1 astrocytes into the lesion. Twenty-eight days after cell transfer, they could illustrate significantly increased remyelination by host oligodendrocytes in the subgroup transplanted with the type-1 astrocytes versus the control group (Franklin et al., 1991). In the Cuprizone model of toxic demyelination, other studies have shown that injured astrocytes secrete several mediators, such as brain-derived neurotrophic factor (BDNF), mitogen platelet-derived growth factor-A (PDGF-A), insulin-like growth factor-1 (IGF-1) and leukaemia inhibitory factor (LIF),

which are known to promote OPC proliferation and differentiation into mature oligodendrocytes, and hence myelin protein synthesis (Baaklini et al., 2019; Moore et al., 2011). Also in the cuprizone mouse model it was recently shown by Houben et al. that astrocytes secrete tissue inhibitor of metalloproteinases-1 (TIMP-1), which supports remyelination by inducing oligodendrocyte differentiation. They could, conversely, show that a deficiency of TIMP-1 hindered remyelination (Houben et al., 2020).

Some studies already tried to integrate these findings on beneficial and harmful roles of astrocytes in demyelinating diseases. The team around Iwama et al. proposed a time dependent shift from “detrimental to protective” functions of astrocytes but also of macrophages and microglia. In a rat model of ODS, the team was able to demonstrate an increase in proinflammatory cytokines secreted by activated microglia in early lesions, accompanied by an increase in general astrocyte numbers. These early-lesion astrocytes initially displayed a reactive morphology and later began to express nerve growth factor and glial cell-derived neurotrophic factor known to support repair mechanisms (Iwama et al., 2011). This is well in line with our findings on astrocyte morphology as well as microglia behavior and morphology as we found less foamy microglia and macrophages in the late-stage lesions besides the astrocytic changes already discussed.

Multiple reviews over the last years supported a much more complex role of astrocytes and, indeed, all cells involved in de-/ remyelinating lesions. Domingues et al., for example, described a binary function of astrocytes in enhancing demyelination by attraction of microglia/macrophages and secretion of proinflammatory cytokines, but as well in remyelination. Among others, remyelination is supported by secretion

of growth factors but seems to depend on the microenvironment of and distance to the lesion itself (Domingues et al., 2016).

Later, Baaklini et al. supported the binary role of astrocytes and the complex interplay with microglia/macrophages in promoting or inhibiting remyelination directly and indirectly. Both reviews described different phenotypes of astrocytes that either induce and perpetuate demyelination/inflammation by hindering OPC differentiation and remyelination in MS or support remyelination by secreting growth factors (Baaklini et al., 2019).

Generally, it is known that the interdependence and cross-talk of astrocytes, oligodendrocytes and also microglia in the CNS plays a pivotal role in myelination (Domingues et al., 2016; Zuchero & Barres, 2015). Hence, interaction of astrocytes and oligodendrocytes via electric as well as metabolic coupling, gap junctions and their close contact might be the basis of their closely linked depletion-recovery curves.

While Menichella et al. demonstrated the general importance of oligodendrocyte connexins for normal CNS myelination during development (Menichella et al., 2003), research teams around Lutz et al. and Li et al. proved astrocyte-oligodendrocyte interdependence essential for myelination by demonstrating functional and lethal consequences of disturbance in their communication via gap junctions and connexins in knock-out mice (Li et al., 2014; Lutz et al., 2009). Recent reviews on the role of astrocytes in (re-) myelination by Molina-Gonzalez et al. and Rawji et al. confirmed that astrocytes not only communicate intensely with oligodendrocytes but also with immune cells and microglia to orchestrate myelination, white matter health in general

but especially remyelination following injury (Molina-Gonzalez & Miron, 2019; Rawji et al., 2020).

Of note, also activated microglia and macrophages play an important part not only in lesion induction but also in its regeneration. Microglia/macrophages seem to serve a more complex role in de-/ and remyelination which is yet incompletely understood. It is well established that microglia secrete proinflammatory cytokines that perpetuate demyelination. Additionally, relatively recent research found that microglia influence astrocytes and are even able to induce a phenotypic shift towards a neurotoxic phenotype that is then able to induce apoptosis in oligodendrocytes (Liddelow et al., 2017).

On the other hand, microglia/macrophages aid in the clearance of myelin debris, enable OPC recruitment, secrete growth factors and seem to influence the extracellular matrix (Baaklini et al., 2019). Some of the molecules secreted by macrophages/microglia, e.g. activin A, insulin-like growth factor 1 (IGF1), galectin 3, tumour necrosis factor (TNF) and Interleukin 1 beta (IL-1 β), promoted OPC recruitment and remyelination in various experiments and are thus essential for oligodendrocyte differentiation during remyelination (Lloyd & Miron, 2019; Miron et al., 2013; Voß et al., 2012). Recent research postulates the presence of specific phenotypes of microglia at certain stages of lesion evolution. First, a proinflammatory subtype (M1), responsible for OPC recruitment and clearance of debris and later at initiation of remyelination a switch to the pro-remyelinating/anti-inflammatory phenotype (M2) that supports remyelination (Lloyd & Miron, 2019; Miron et al., 2013).

Clinical data on humans with histopathological confirmation are difficult to obtain. However, recently evidence of remyelinated axons in a patient with subclinical

longstanding ODS has been brought forward (Haynes et al., 2018). On autopsy, thinly myelinated sheaths weakly positive for PLP were found within the demyelinated lesion. The authors figured that this remyelination could be the cause of the lack of symptoms in this patient. This shows that neurological recovery is, indeed, possible in human ODS and there might be a number of unrecognized subclinical cases.

In our study, the late-stage lesions partly demonstrated pale LFB staining, an indicator for remyelination. Therefore, our data is in line with recent research and literature on the topic of lesion evolution in ODS, and our staging of the human cases is plausible in the light of astrocyte, oligodendrocyte, and microglia behaviour as well as de- and remyelination.

Nonetheless, remyelination as one goal of lesion repair in CPM requires a complex interaction of astrocytes, oligodendrocyte precursors and mature oligodendrocytes as well as microglia/macrophages within the CNS (Baaklini et al., 2019; Domingues et al., 2016; Iwama et al., 2011; Liddelow et al., 2017; Miron et al., 2013). It is likely that astrocytes provide different functions at different stages of lesion evolution. However, the interplay of these cells and factors involved are of immense and current research interest and are beyond the scope of this work.

	Astrocytes	Oligodendrocytes	Macrophages/ Microglia	Myelin
early-stage	<ul style="list-style-type: none"> • low density • repopulation by bipolar astrocytes • absence of AQP4 immunoreactivity 	<ul style="list-style-type: none"> • low density • signs of injury like chromatin hypercondensation / nuclear fragmentation 	<ul style="list-style-type: none"> • extensive infiltration by activated/ foamy microglia/macrophages • phagocytosis of myelin 	<ul style="list-style-type: none"> • demyelination
intermediate-stage	<ul style="list-style-type: none"> • increased densities • bipolar, and ramified astrocytes • mostly AQP4 negative 	<ul style="list-style-type: none"> • low density • signs of injury like chromatin hypercondensation / nuclear fragmentation 	<ul style="list-style-type: none"> • moderate densities • partially foamy 	<ul style="list-style-type: none"> • reduced
late-stage	<ul style="list-style-type: none"> • almost normal densities • reactive morphology • AQP4 positive • less bipolar cells 	<ul style="list-style-type: none"> • low density • abnormal morphology with swollen cell bodies 	<ul style="list-style-type: none"> • less activated microglia/ macrophages • less phagocytic morphology 	<ul style="list-style-type: none"> • pale, remyelinated

Fig. 20: Lesion evolution of human CPM. Concise overview of histopathological changes in early-, intermediate- and late-stage CPM lesions regarding main cell entities involved.

4.5 Summary, interpretation and limitations of our study

We analysed the post-mortem histopathological data of 20 human CPM cases and, consistent with the literature, demonstrated a high percentage of patients with chronic alcoholism and/ or liver transplantation with 76.5% and 6.3% respectively. This is in line with the previously published work by Gocht et al. derived from the same sources our study used. Further, the patient data regarding age, sex and comorbidities match those described in previously published papers (Gocht & Colmant, 1987). In our human cohort, we found extensive and confluent demyelinated lesions in LFB/PAS staining that were confirmed by immunohistochemistry for the myelin proteins MBP, PLP, MOG and MAG.

Research into human CPM is precluded by several limitations. On the one hand, human pontine samples only represent a snapshot of lesion development and are intrinsically coupled to a fatal clinical outcome. Thus, it is justified to assume a relatively narrow time-window of lesion development within all published cases of CPM. Moreover, it is likely that very early and very late-stage cases in patients with complete clinical recovery are underrepresented. Additionally, multiple comorbidities and previous medical manipulations frequently found in CPM patients may mask the pathophysiological interpretation as these might influence not only the extent of lesion formation but also the regenerative capacity of lesions. Further, even though advancements in MRI technology may aid diagnosis, radiologically determined lesions do not directly correlate with clinical manifestation or outcome in CPM which leaves the timing of lesion initiation uncertain (Graff-Radford et al., 2011; Lambeck et al., 2019). However, our results may also be affected by selection bias, as our data can only represent a snapshot of lesion development.

In the light of the mentioned limitations, we, however, are certain that astrocytes play a crucial part in the development of CPM lesions as well as in their repair. We demonstrated a high density of bipolar astrocytes in the early- and intermediate cohort which suggests a role in regeneration and lesion repair.

In alignment with the literature, our data support the hypothesis that ODS is multifactorial and likely to occur in patients with conditions that predispose to deficiencies in neuronal and glial energy supply (Ashrafian & Davey, 2001). This hypothesis is backed by current research as well as our clinical data on patients suffering from malnutrition, alcoholism and or liver disease and hypoglycaemia (Ashrafian & Davey, 2001; Hurley et al., 2011; Iwama et al., 2011; Kleinschmidt-

Demasters et al., 2006; Lambeck et al., 2019; Nicaise et al., 2019; Popescu et al., 2013).

5 Conclusion and Outlook

This thesis forms part of a larger study that involved the neuropathology departments at the “*University Medical Center Göttingen*”, the “*University hospital in Leipzig*” as well as the neuropathology department at the “*Hospital Kassel*”. We analysed astrocyte and oligodendrocyte densities as well as morphology in histopathological slides of CPM lesions in human pontine samples. Moreover, we analysed macrophages, microglia and expression of aquaporin-4. Our study supports the hypothesis of an early osmotic damage to astrocytes in human CPM lesions and is in line with previously published work and disease mechanisms described in animal models.

From our data we infer the following time course of lesion formation in human ODS: Damage to and loss of astrocytes/AQP4-rich astroglial endfeet in response to osmotic stress, closely followed by loss of oligodendrocytes, possibly in part mediated by the release of toxic cytokines from damaged astrocytes as well as by activated microglia/macrophages, and finally loss of myelin integrity cumulating in myelin phagocytosis and loss. The repopulation with bipolar astrocytes and re-expression of AQP4 is, then, closely followed by the regeneration of oligodendrocytes and reappearance of thinly myelinated axons. However, oligodendrocyte densities, as well as myelin, seem to remain below pre-insult and perilesional levels.

Further studies are needed to integrate the knowledge on the interdependence of astrocytes, oligodendrocytes and microglia/macrophages with clinical data on

comorbidities and also new diagnostic options to be able to develop an in-depth understanding of the pathomechanism underlying tissue damage in CPM. This is essential to develop effective treatment options for patients suffering from osmotic demyelination syndromes.

6 Bibliography

- ADAMS, R. D., VICTOR, M., & MANCALL, E. L. (1959). Central pontine myelinolysis: A hitherto undescribed disease occurring in alcoholic and malnourished patients. *A.M.A. Archives of Neurology and Psychiatry*, *81*(2), 154–172.
- Akaishi, T., & Sakuma, Y. (1990). Estrogen-induced modulation of hypothalamic osmoregulation in female rats. *The American Journal of Physiology*, *258*(4 Pt 2), R924-929. <https://doi.org/10.1152/ajpregu.1990.258.4.R924>
- Baaklini, C. S., Rawji, K. S., Duncan, G. J., Ho, M. F. S., & Plemel, J. R. (2019). Central Nervous System Remyelination: Roles of Glia and Innate Immune Cells. *Frontiers in Molecular Neuroscience*, *12*, 225. <https://doi.org/10.3389/fnmol.2019.00225>
- Back, S. A., Tuohy, T. M. F., Chen, H., Wallingford, N., Craig, A., Struve, J., Luo, N. L., Banine, F., Liu, Y., Chang, A., Trapp, B. D., Bebo, Bruce F., Rao, M. S., & Sherman, L. S. (2005). Hyaluronan accumulates in demyelinated lesions and inhibits oligodendrocyte progenitor maturation. *Nature Medicine*, *11*(9), 966–972. <https://doi.org/10.1038/nm1279>
- Baker, E. A., Tian, Y., Adler, S., & Verbalis, J. G. (2000). Blood-brain barrier disruption and complement activation in the brain following rapid correction of chronic hyponatremia. *Experimental Neurology*, *165*(2), 221–230. <https://doi.org/10.1006/exnr.2000.7474>
- Bannerman, P., Horiuchi, M., Feldman, D., Hahn, A., Itoh, A., See, J., Jia, Z. P., Itoh, T., & Pleasure, D. (2007). GluR2-free α -amino-3-hydroxy-5-methyl-4-isoxazolepropionate receptors intensify demyelination in experimental

- autoimmune encephalomyelitis. *Journal of Neurochemistry*, 102(4), 1064–1070. <https://doi.org/10.1111/j.1471-4159.2007.04612.x>
- Bouchat, J., Couturier, B., Marneffe, C., Gankam-Kengne, F., Balau, B., De Swert, K., Brion, J.-P., Poncelet, L., Gilloteaux, J., & Nicaise, C. (2018). Regional oligodendrocytopathy and astrocytopathy precede myelin loss and blood-brain barrier disruption in a murine model of osmotic demyelination syndrome. *Glia*, 66(3), 606–622. <https://doi.org/10.1002/glia.23268>
- Brambilla, R., Persaud, T., Hu, X., Karmally, S., Shestopalov, V. I., Dvorianchikova, G., Ivanov, D., Nathanson, L., Barnum, S. R., & Bethea, J. R. (2009). Transgenic Inhibition of Astroglial NF- κ B Improves Functional Outcome in Experimental Autoimmune Encephalomyelitis by Suppressing Chronic Central Nervous System Inflammation. *The Journal of Immunology*, 182(5), 2628. <https://doi.org/10.4049/jimmunol.0802954>
- Brück, W., Popescu, B., Lucchinetti, C. F., Markovic-Plese, S., Gold, R., Thal, D. R., & Metz, I. (2012). Neuromyelitis optica lesions may inform multiple sclerosis heterogeneity debate. *Annals of Neurology*, 72(3), 385–394. <https://doi.org/10.1002/ana.23621>
- Cammer, W. (2000). Effects of TNF α on immature and mature oligodendrocytes and their progenitors in vitro. *Brain Research*, 864(2), 213–219. [https://doi.org/10.1016/s0006-8993\(00\)02178-8](https://doi.org/10.1016/s0006-8993(00)02178-8)
- Choi, S. S., Lee, H. J., Lim, I., Satoh, J., & Kim, S. U. (2014). Human astrocytes: Secretome profiles of cytokines and chemokines. *PloS One*, 9(4), e92325. <https://doi.org/10.1371/journal.pone.0092325>

-
- Correale, J., & Farez, M. F. (2015). The Role of Astrocytes in Multiple Sclerosis Progression. *Frontiers in Neurology*, 6, 180. <https://doi.org/10.3389/fneur.2015.00180>
- DeLuca, G. C., Nagy, Z., Esiri, M. M., & Davey, P. (2002). Evidence for a role for apoptosis in central pontine myelinolysis. *Acta Neuropathologica*, 103(6), 590–598. <https://doi.org/10.1007/s00401-001-0508-2>
- Domingues, H. S., Portugal, C. C., Socodato, R., & Relvas, J. B. (2016). Oligodendrocyte, Astrocyte, and Microglia Crosstalk in Myelin Development, Damage, and Repair. *Frontiers in Cell and Developmental Biology*, 4, 71. <https://doi.org/10.3389/fcell.2016.00071>
- Eccles, D., Li, N., Handwerker, R., Maishman, T., Copson, E., Durcan, L. T., Gerty, S. M., Jones, L., Evans, D., Haywood, L., & Campbell, I. (2015). Genetic testing in a cohort of young patients with HER2 amplified breast cancer. *Annals of Oncology: Official Journal of the European Society for Medical Oncology / ESMO*, 27. <https://doi.org/10.1093/annonc/mdv592>
- Fraser, C. L., Kucharczyk, J., Arieff, A. I., Rollin, C., Sarnacki, P., & Norman, D. (1989). Sex differences result in increased morbidity from hyponatremia in female rats. *The American Journal of Physiology*, 256(4 Pt 2), R880-885. <https://doi.org/10.1152/ajpregu.1989.256.4.R880>
- Gankam Kengne, F., Nicaise, C., Soupart, A., Boom, A., Schiettecatte, J., Pochet, R., Brion, J. P., & Decaux, G. (2011). Astrocytes are an early target in osmotic demyelination syndrome. *Journal of the American Society of Nephrology: JASN*, 22(10), 1834–1845. PubMed. <https://doi.org/10.1681/ASN.2010111127>
- Gankam-Kengne, F., Couturier, B. S., Soupart, A., Brion, J. P., & Decaux, G. (2017). Osmotic Stress-Induced Defective Glial Proteostasis Contributes to Brain

-
- Demyelination after Hyponatremia Treatment. *Journal of the American Society of Nephrology: JASN*, 28(6), 1802–1813. PubMed.
<https://doi.org/10.1681/ASN.2016050509>
- Gard, A. L., Burrell, M. R., Pfeiffer, S. E., Rudge, J. S., & Williams, W. C. 2nd. (1995). Astroglial control of oligodendrocyte survival mediated by PDGF and leukemia inhibitory factor-like protein. *Development (Cambridge, England)*, 121(7), 2187–2197.
- Gocht, A., & Colmant, H. J. (1987). Central pontine and extrapontine myelinolysis: A report of 58 cases. *Clinical Neuropathology*, 6(6), 262–270.
- Hammond, T. R., Gadea, A., Dupree, J., Kerninon, C., Nait-Oumesmar, B., Aguirre, A., & Gallo, V. (2014). Astrocyte-derived endothelin-1 inhibits remyelination through notch activation. *Neuron*, 81(3), 588–602.
<https://doi.org/10.1016/j.neuron.2013.11.015>
- Houben, E., Janssens, K., Hermans, D., Vandooren, J., Van den Haute, C., Schepers, M., Vanmierlo, T., Lambrichts, I., van Horssen, J., Baekelandt, V., Opdenakker, G., Baron, W., Broux, B., Slaets, H., & Hellings, N. (2020). Oncostatin M-induced astrocytic tissue inhibitor of metalloproteinases-1 drives remyelination. *Proceedings of the National Academy of Sciences of the United States of America*, 117(9), 5028–5038.
<https://doi.org/10.1073/pnas.1912910117>
- Huang, D., Wang, J., Kivisakk, P., Rollins, B. J., & Ransohoff, R. M. (2001). Absence of Monocyte Chemoattractant Protein 1 in Mice Leads to Decreased Local Macrophage Recruitment and Antigen-Specific T Helper Cell Type 1 Immune Response in Experimental Autoimmune Encephalomyelitis. *Journal of*

-
- Experimental Medicine*, 193(6), 713–726.
<https://doi.org/10.1084/jem.193.6.713>
- Hurley, R. A., Filley, C. M., & Taber, K. H. (2011). Central Pontine Myelinolysis: A Metabolic Disorder of Myelin. *The Journal of Neuropsychiatry and Clinical Neurosciences*, 23(4), 369–374. <https://doi.org/10.1176/jnp.23.4.jnp369>
- Iwama, S., Sugimura, Y., Suzuki, H., Suzuki, H., Murase, T., Ozaki, N., Nagasaki, H., Arima, H., Murata, Y., Sawada, M., & Oiso, Y. (2011). Time-dependent changes in proinflammatory and neurotrophic responses of microglia and astrocytes in a rat model of osmotic demyelination syndrome. *Glia*, 59(3), 452–462. <https://doi.org/10.1002/glia.21114>
- Junker, A., Wozniak, J., Voigt, D., Scheidt, U., Antel, J., Wegner, C., Brück, W., & Stadelmann, C. (2020). Extensive subpial cortical demyelination is specific to multiple sclerosis. *Brain Pathology (Zurich, Switzerland)*, 30(3), 641–652. <https://doi.org/10.1111/bpa.12813>
- Kleinschmidt-DeMasters, B. K., & Norenberg, M. D. (1981). Rapid correction of hyponatremia causes demyelination: Relation to central pontine myelinolysis. *Science (New York, N.Y.)*, 211(4486), 1068–1070.
- Kleinschmidt-Demasters, B. K., Rojiani, A. M., & Filley, C. M. (2006). Parr. *Journal of Neuropathology and Experimental Neurology*, 65(1), 1–11.
- Li, T., Giaume, C., & Xiao, L. (2014). Connexins-mediated glia networking impacts myelination and remyelination in the central nervous system. *Molecular Neurobiology*, 49(3), 1460–1471. <https://doi.org/10.1007/s12035-013-8625-1>
- Liddel, S. A., Guttenplan, K. A., Clarke, L. E., Bennett, F. C., Bohlen, C. J., Schirmer, L., Bennett, M. L., Münch, A. E., Chung, W.-S., Peterson, T. C., Wilton, D. K., Frouin, A., Napier, B. A., Panicker, N., Kumar, M., Buckwalter,

-
- M. S., Rowitch, D. H., Dawson, V. L., Dawson, T. M., ... Barres, B. A. (2017). Neurotoxic reactive astrocytes are induced by activated microglia. *Nature*, *541*(7638), 481–487. <https://doi.org/10.1038/nature21029>
- Lloyd, A. F., & Miron, V. E. (2019). The pro-remyelination properties of microglia in the central nervous system. *Nature Reviews Neurology*. <https://doi.org/10.1038/s41582-019-0184-2>
- Lohrberg, M., Winkler, A., Franz, J., van der Meer, F., Ruhwedel, T., Sirmipilatz, N., Dadarwal, R., Handwerker, R., Esser, D., Wiegand, K., Hagel, C., Gocht, A., König, F. B., Boretius, S., Möbius, W., Stadelmann, C., & Barrantes-Freer, A. (2020). Lack of astrocytes hinders parenchymal oligodendrocyte precursor cells from reaching a myelinating state in osmolyte-induced demyelination. *Acta Neuropathologica Communications*, *8*(1), 224. <https://doi.org/10.1186/s40478-020-01105-2>
- Lutz, S. E., Zhao, Y., Gulinello, M., Lee, S. C., Raine, C. S., & Brosnan, C. F. (2009). Deletion of astrocyte connexins 43 and 30 leads to a dysmyelinating phenotype and hippocampal CA1 vacuolation. *The Journal of Neuroscience: The Official Journal of the Society for Neuroscience*, *29*(24), 7743–7752. <https://doi.org/10.1523/JNEUROSCI.0341-09.2009>
- Mader, S., & Brimberg, L. (2019). Aquaporin-4 Water Channel in the Brain and Its Implication for Health and Disease. *Cells*, *8*(2). <https://doi.org/10.3390/cells8020090>
- Maria Teresa Gentile. (2018). Introductory Chapter: The Importance of Astrocytes in the Research of CNS Diseases. In Luca Colucci D'Amato ED1 - Maria Teresa Gentile ED2 - Luca Colucci D'Amato (Ed.), *Astrocyte* (p. Ch. 1). IntechOpen. <https://doi.org/10.5772/intechopen.74710>

-
- Menichella, D., A Goodenough, D., Sirkowski, E., Scherer, S., & Paul, D. (2003). *Connexins Are Critical for Normal Myelination in the CNS* (Vol. 23). <https://doi.org/10.1523/JNEUROSCI.23-13-05963.2003>
- Miron, V. E., Boyd, A., Zhao, J.-W., Yuen, T. J., Ruckh, J. M., Shadrach, J. L., van Wijngaarden, P., Wagers, A. J., Williams, A., Franklin, R. J. M., & ffrench-Constant, C. (2013). M2 microglia and macrophages drive oligodendrocyte differentiation during CNS remyelination. *Nature Neuroscience*, *16*(9), 1211–1218. <https://doi.org/10.1038/nn.3469>
- Molina-Gonzalez, I., & Miron, V. E. (2019). Astrocytes in myelination and remyelination. *Neuroscience Letters*, *713*, 134532. <https://doi.org/10.1016/j.neulet.2019.134532>
- Moore, C. S., Abdullah, S. L., Brown, A., Arulpragasam, A., & Crocker, S. J. (2011). How factors secreted from astrocytes impact myelin repair. *Journal of Neuroscience Research*, *89*(1), 13–21. <https://doi.org/10.1002/jnr.22482>
- Nicaise, C., Marneffe, C., Bouchat, J., & Gilloteaux, J. (2019). Osmotic Demyelination: From an Oligodendrocyte to an Astrocyte Perspective. *International Journal of Molecular Sciences*, *20*(5), 1124. PubMed. <https://doi.org/10.3390/ijms20051124>
- Parratt, J. D. E., & Prineas, J. W. (2010). Neuromyelitis optica: A demyelinating disease characterized by acute destruction and regeneration of perivascular astrocytes. *Multiple Sclerosis (Houndmills, Basingstoke, England)*, *16*(10), 1156–1172. <https://doi.org/10.1177/1352458510382324>
- Ponath, G., Park, C., & Pitt, D. (2018). The Role of Astrocytes in Multiple Sclerosis. *Frontiers in Immunology*, *9*, 217. <https://doi.org/10.3389/fimmu.2018.00217>

-
- Popescu, B. F. G., Bunyan, R. F., Guo, Y., Parisi, J. E., Lennon, V. A., & Lucchinetti, C. F. (2013). Evidence of aquaporin involvement in human central pontine myelinolysis. *Acta Neuropathologica Communications*, *1*, 40. <https://doi.org/10.1186/2051-5960-1-40>
- Prineas, J. W., & Lee, S. (2019). Multiple Sclerosis: Destruction and Regeneration of Astrocytes in Acute Lesions. *Journal of Neuropathology and Experimental Neurology*, *78*(2), 140–156. <https://doi.org/10.1093/jnen/nly121>
- Pringle, N., Collarini, E. J., Mosley, M. J., Heldin, C. H., Westermark, B., & Richardson, W. D. (1989). PDGF A chain homodimers drive proliferation of bipotential (O-2A) glial progenitor cells in the developing rat optic nerve. *The EMBO Journal*, *8*(4), 1049–1056.
- Rash, J. E. (2010). Molecular disruptions of the panglial syncytium block potassium siphoning and axonal saltatory conduction: Pertinence to neuromyelitis optica and other demyelinating diseases of the central nervous system. *Neuroscience*, *168*(4), 982–1008. <https://doi.org/10.1016/j.neuroscience.2009.10.028>
- Rawji, K. S., Gonzalez Martinez, G. A., Sharma, A., & Franklin, R. J. M. (2020). The Role of Astrocytes in Remyelination. *Trends in Neurosciences*, *43*(8), 596–607. <https://doi.org/10.1016/j.tins.2020.05.006>
- Ryu, H. J., Kim, J.-E., Yeo, S.-I., Kim, D.-W., Kwon, O.-S., Choi, S. Y., & Kang, T.-C. (2011). F-actin depolymerization accelerates clasmatodendrosis via activation of lysosome-derived autophagic astroglial death. *Brain Research Bulletin*, *85*(6), 368–373. <https://doi.org/10.1016/j.brainresbull.2011.05.007>

-
- Singh, T. D., Fugate, J. E., & Rabinstein, A. A. (2014). Central pontine and extrapontine myelinolysis: A systematic review. *European Journal of Neurology*, *21*(12), 1443–1450. <https://doi.org/10.1111/ene.12571>
- Stadelmann, C., Timmler, S., Barrantes-Freer, A., & Simons, M. (2019). Myelin in the Central Nervous System: Structure, Function, and Pathology. *Physiological Reviews*, *99*(3), 1381–1431. <https://doi.org/10.1152/physrev.00031.2018>
- Talbott, J. F., Loy, D. N., Liu, Y., Qiu, M. S., Bunge, M. B., Rao, M. S., & Whittemore, S. R. (2005). Endogenous Nkx2.2+/Olig2+ oligodendrocyte precursor cells fail to remyelinate the demyelinated adult rat spinal cord in the absence of astrocytes. *Experimental Neurology*, *192*(1), 11–24. <https://doi.org/10.1016/j.expneurol.2004.05.038>
- Traka, M., Podojil, J. R., McCarthy, D. P., Miller, S. D., & Popko, B. (2016). Oligodendrocyte death results in immune-mediated CNS demyelination. *Nature Neuroscience*, *19*(1), 65–74. PubMed. <https://doi.org/10.1038/nn.4193>
- Voß, E. V., Škuljec, J., Gudi, V., Skripuletz, T., Pul, R., Trebst, C., & Stangel, M. (2012). Characterisation of microglia during de- and remyelination: Can they create a repair promoting environment? *Assessment of Gene Expression in Neuropsychiatric Disease*, *45*(1), 519–528. <https://doi.org/10.1016/j.nbd.2011.09.008>
- Weil, M.-T., Mobius, W., Winkler, A., Ruhwedel, T., Wrzos, C., Romanelli, E., Bennett, J. L., Enz, L., Goebels, N., Nave, K.-A., Kerschensteiner, M., Schaeren-Wiemers, N., Stadelmann, C., & Simons, M. (2016). Loss of Myelin Basic Protein Function Triggers Myelin Breakdown in Models of Demyelinating Diseases. *Cell Reports*, *16*(2), 314–322. <https://doi.org/10.1016/j.celrep.2016.06.008>

-
- Wrzos, C., Winkler, A., Metz, I., Kayser, D. M., Thal, D. R., Wegner, C., Brück, W., Nessler, S., Bennett, J. L., & Stadelmann, C. (2014). Early loss of oligodendrocytes in human and experimental neuromyelitis optica lesions. *Acta Neuropathologica*, 127(4), 523–538. PubMed. <https://doi.org/10.1007/s00401-013-1220-8>
- Zou, L.-B., Shi, S., Zhang, R.-J., Wang, T.-T., Tan, Y.-J., Zhang, D., Fei, X.-Y., Ding, G.-L., Gao, Q., Chen, C., Hu, X.-L., Huang, H.-F., & Sheng, J.-Z. (2013). Aquaporin-1 plays a crucial role in estrogen-induced tubulogenesis of vascular endothelial cells. *The Journal of Clinical Endocrinology and Metabolism*, 98(4), E672-682. <https://doi.org/10.1210/jc.2012-4081>

7 List of Tables

Table 1: Factors predisposing to the development of ODS.....	14
Table 2: Embedding protocol – Excelsior AS1 & AS2 (Einbettungsprozess des Institus für Neuropathologie, Universitätsmedizin Göttingen, valid since last revision on 26 th Feb, 2019).....	24
Table 3: Antibodies used for IHC and/or immunofluorescence.....	28
Table 4: Clinical information on CPM patients.....	33
Table 5: Characteristics of patients with CPM.....	34

8 List of Figures

- Fig. 1: Schematic representation of changes in the brain as response to osmotic stress.....
- Fig. 2: Principle of IHC- direct versus indirect method.....
- Fig. 3: Representative microphotographs of CPM lesions visualized by LFB/PAS staining.....
- Fig. 4: Features of early-stage CPM.....
- Fig. 5: Features of intermediate-stage CPM.....
- Fig. 6: Features of late-stage CPM.....
- Fig. 7: Astrocyte density in early-, mid-stage and late-stage human CPM.....
- Fig. 8: Astrocyte density across early-, mid-stage and late-stage human CPM.....
- Fig. 9: Bipolar astrocyte in an early human CPM lesion.....
- Fig. 10: Bipolar astrocytes in early, intermediate-stage and late-stage human CPM.
- Fig. 11: Early, intermediate and late-stage CPM lesions stained for GFAP.....
- Fig. 12: Oligodendrocyte density in early-, intermediate- and late-stage human CPM.
- Fig. 13: Oligodendrocyte density in early CPM lesions.....
- Fig. 14: Correlation of astrocyte and oligodendrocyte density in early lesions.....
- Fig. 15: Astrocyte and Oligodendrocyte density in early, intermediate- and late-stage lesions.....
- Fig. 16: Density of KiM1P positive macrophages/activated microglia in early-, intermediate- and late-stage human CPM.....
- Fig. 17: Macrophage infiltration into human CPM lesions.

-
- Fig. 18: Early-stage CPM lesion with myelin-phagocytosing macrophages.....
- Fig. 19: Density of proliferating Iba1/Ki67 double positive macrophages/microglia in early-, intermediate- and late-stage human CPM.
- Fig. 20: Lesion evolution of human CPM.....

9.3 Acknowledgements

An dieser Stelle möchte ich allen danken, die mir sowohl den Beginn als auch die Vollendung meiner Doktorarbeit ermöglicht haben:

Allen voran Frau Prof. Stadelmann-Nessler, die mir die Möglichkeit gab, meine Promotionsarbeit in ihrem Arbeitskreis zu beginnen und die mich mit ihrer Leidenschaft und Energie für ihr Fachgebiet immer wieder inspiriert hat. Ihr Feedback und ihre konstruktive Kritik haben mich immer wieder motiviert weiter zu denken und noch ein Schippchen mehr zu geben.

Weiterhin danke ich Herrn Prof. Dr. med. Wolf Müller dafür, dass ich meine Dissertation in seiner Klinik fortführen durfte.

Natürlich geht besonderer Dank ebenfalls an Dr. Alonso Barrantes-Freer, der es mir ermöglicht hat mit meiner Promotion fortzufahren, als sie kurz ins Wanken geriet und mir die Grundsätze der neuropathologischen Arbeit nahebrachte. Auch sein regelmäßiges Feedback hat es mir ermöglicht, die Arbeit immer wieder ein Stückchen zu verbessern.

Weiterhin danke ich Frau Dr. Fatima B. König für konstanten Rat, Motivation und Fürsprache weit über die Promotion hinaus. Ohne sie wäre ich nicht dort, wo ich gerade bin -weder wissenschaftlich, noch im Bezug auf meine weitere Zukunftsplanung.

Nicht zu vergessen ist die immense Unterstützung, die ich von Melanie Lohrberg, Anne Winkler und Franziska van der Meer in den (vor-) letzten Zügen meiner Dissertation erfahren durfte. Sie haben mich in besonderem Maße in den Feinheiten der Discussion sowie bei der Erstellung der Grafiken und Figures beraten. Hier kann ich meine Wertschätzung auch schwer in Worte fassen.

Ich denke, der persönliche Dank wird der umwerfenden Unterstützung und Motivation, die ich über die Jahre erfahren durfte am meisten gerecht werden!

Letzendlich bedanke ich mich bei meinem großartigen Mann, Steffen, der mir über die gesamte Zeit enormen Halt, Motivation und Nachsicht für die vielen Monologe und Stunden am Mikroskop entgegengebracht hat.

Danke!